

# Solutions to Problems

## *Theory of Dislocations*, 3rd edition

Student Version 11/2020

PM Anderson, JP Hirth, and J Lothe

---

**Background:** These solutions were developed by JP Hirth and PM Anderson to provide students with answers to a portion of over 200 problems from the textbook, underscoring key principles and demonstrating worked examples of the application of dislocation theory. The complete set of solutions is available to instructors through the [publisher website](#). Problems with the entry “MATLAB” at the beginning of the answer indicate that a supporting MATLAB file is available through the publisher website to aid in computing the answer. In many cases, extended answers are provided to both teach and expand the context of the application or theory. Red text in the question statement indicates a correction to the published question in the textbook. Suggestions or corrections to answers can be sent to [anderson.1@osu.edu](mailto:anderson.1@osu.edu).

CHAPTER 1: INTRODUCTORY MATERIAL	2
CHAPTER 2: ELASTICITY	5
CHAPTER 3: THEORY OF STRAIGHT DISLOCATIONS	7
CHAPTER 4: THEORY OF CURVED DISLOCATIONS	12
CHAPTER 5: APPLICATIONS TO DISLOCATION INTERACTIONS	14
CHAPTER 6: APPLICATIONS TO SELF ENERGIES	18
CHAPTER 7: DISLOCATIONS AT HIGH VELOCITIES	24
CHAPTER 8: THE INFLUENCE OF LATTICE PERIODICITY	27
CHAPTER 9: SLIP SYSTEMS OF PERFECT DISLOCATIONS	30
CHAPTER 10: PARTIAL DISLOCATIONS IN FCC METALS	34
CHAPTER 11: PARTIAL DISLOCATIONS IN OTHER STRUCTURES	38
CHAPTER 12: DISLOCATIONS IN IONIC CRYSTALS	40
CHAPTER 13: DISLOCATIONS IN ANISOTROPIC ELASTIC MEDIA	42
CHAPTER 14: EQUILIBRIUM DEFECT CONCENTRATIONS	45
CHAPTER 15: DIFFUSIVE GLIDE AND CLIMB PROCESSES	50
CHAPTER 16: GLIDE OF JOGGED DISLOCATIONS	54
CHAPTER 17: DISLOCATION MOTION IN VACANCY SUPERSATURATIONS	56
CHAPTER 18: EFFECTS OF SOLUTE ATOMS ON DISLOCATION MOTION	59
CHAPTER 19: GRAIN BOUNDARIES AND INTERFACES	62
CHAPTER 20: DISLOCATION SOURCES	65
CHAPTER 21: DISLOCATION PILEUPS	69
CHAPTER 22: DISLOCATION INTERSECTIONS AND BARRIERS	71
CHAPTER 23: DEFORMATION TWINNING	73

## CHAPTER 1: INTRODUCTORY MATERIAL

**Description:** These problems examine the physics of why dislocations facilitate deformation of crystals, surface ledges created by their motion, identification of vacancy and interstitial loops, and construction of Burgers circuits.

- 1.1 Discuss qualitatively how the presence of edge dislocations (Figure 1.4) can account for the shear of crystals at stresses much less than  $\sigma_{\text{theor}}$ . Is the same explanation valid for screw dislocations?

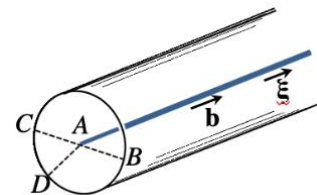
- 1.2 A screw dislocation with  $\mathbf{b} \parallel \xi$  lies along the axis of the cylinder in Figure 1.28 (See accompanying figure).

a. If the ledge is along  $AB$ , is it recessing or overhanging?

b. If the ledge is along  $AC$ , is it recessing or overhanging?

c. Is there any restriction on the ledge position? Could it be positioned at  $AD$ ?

d. Construct a rule to specify the sign of the ledge (recessing or overhanging) in terms of  $\mathbf{b}$  and  $\xi$ . *Hint:* Develop a right-hand or left-hand rule.

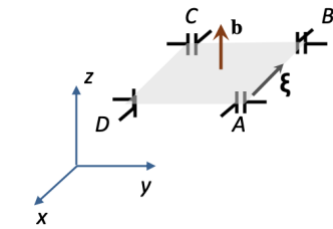


Problem 1.2. Figure 1.28. A screw dislocation lying along the axis of a cylinder.

1.3 Form a closed, planar square *interstitial* dislocation loop by inserting one atomic layer within the loop. Form a *vacancy* loop by removing an atomic layer. Specify the resulting dislocations in terms of  $\mathbf{b}$  and  $\xi$ . Develop a rule that uses  $\mathbf{b}$  and  $\xi$  to distinguish between interstitial and vacancy loops.

1.4★ Insert one of the loops of Prob. 1.3 into a cube of material and orient it parallel to one of the cube faces. Sketch the response of the loop to an imposed shear stress on the cube faces. Consider the three possible components of shear stress.

Consider the adjoining figure showing a vacancy loop  $ABCD$  and Cartesian basis  $xyz$ . Each edge of the square vacancy loop is represented by an edge dislocation with a slip direction and slip plane (e.g., the slip plane for dislocation  $AB$  is parallel to the  $y$ -face). By analogy to Figure 1.19a,b, a shear stress – represented by a force parallel to the slip direction (e.g., along  $z$ ) and applied to a cube face parallel to a slip plane (e.g., a plane parallel to the  $y$ -face) – will act to move the dislocation. Therefore, a shear stress  $\sigma_{yz}$  ( $= \sigma_{zy}$ ) will tend to move dislocation  $AB$  along the  $z$ -direction and  $CD$  along the  $-z$  direction, and a shear stress  $\sigma_{xz}$  ( $= \sigma_{zx}$ ) will tend to move dislocation  $DA$  along the  $z$ -direction and  $BC$  along the  $-z$  direction.

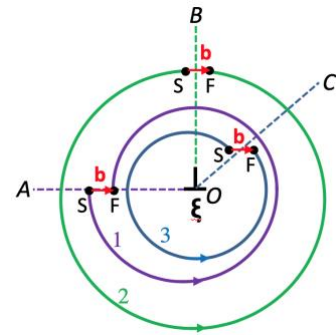


Problem 1.4.

1.5 Extra material can be inserted in Figure 1.19e to produce the edge dislocation in Figure 1.19f. If a tensile stress were applied perpendicular to the extra plane of material, would you expect the dislocation to climb upward or downward?

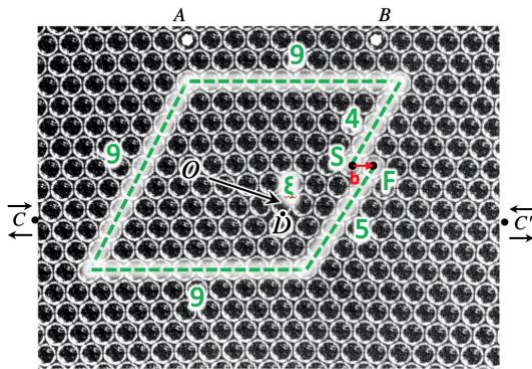
1.6★ The cuts in Figure 1.19 are parallel to cube faces. Show that the dislocations can be formed by a cut on any plane in the crystal. Specifically, form the same dislocations by a cut inclined at  $45^\circ$  to those in the figure.

The adjoining figure show three potential cuts – along  $OA$ ,  $OB$ , and  $OC$  – each of which creates the edge dislocation shown in the center of the figure with line direction  $\xi$  pointing outward and  $\mathbf{b}$  pointing to the right. For the cut  $OA$ , a right-handed Burgers circuit (circuit #1, shown in purple) is constructed in the deformed (dislocated) material. Using the SF/RH convention as detailed in Fig. 1.21, the Burgers vector is defined as the vector from the start (S) to finish (F) points. This is equivalent to the cut in Fig. 1.19b. Likewise, cuts  $OB$  (circuit #2, shown in green) and  $OC$  (circuit #3, shown in blue) can be used. The latter is a cut at 45 degrees and involves both relative opening and shearing of the surfaces along the cut.



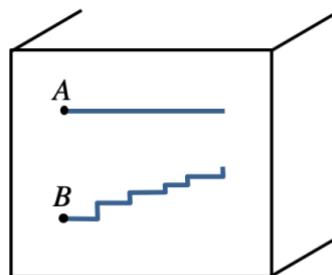
Problem 1.6.

- 1.7 Use a Burgers circuit to determine  $\mathbf{b}$  for the dislocation in the bubble raft of Figure 1.6. Show that the dislocation can be formed by any one of several cuts within the bubble raft, analogous to Prob. 1.6.



Problem 1.7.

- 1.8 Figure 1.29 shows the slip traces along a sample surface caused by motion of two dislocations initially at A and B. Which trace must have a surface ledge? Why?



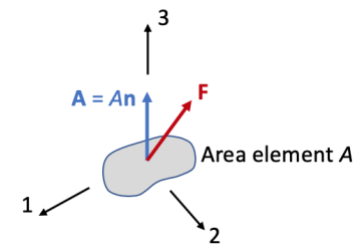
Problem 1.8. Figure 1.29. Slip traces generated where the slip surface intersects a free surface, for two dislocations originally at A and B.

## CHAPTER 2: ELASTICITY

**Description:** These problems examine: the transformation of strain or stress components arising from a change in basis; effects of crystal symmetry on elastic constants; and application of elastic constitutive relations.

- 2.1 Consider a state of plane strain that has  $\epsilon_{xx}$ ,  $\epsilon_{yy}$ , and  $\epsilon_{xy}$  ( $= \epsilon_{yx}$ ) as the only nonzero components of strain. Find the components of strain referred to a coordinate system  $x'y'$  that is rotated an angle  $\phi$  about a common  $z$  axis.
- 2.2 Consider a state of strain that has  $\epsilon_{xz}$  ( $= \epsilon_{zx}$ ) and  $\epsilon_{yz}$  ( $= \epsilon_{zy}$ ) as the only nonvanishing components. Find the components of strains referred to a coordinate system  $x'y'$  that is rotated an angle  $\phi$  about a common  $z$  axis.
- 2.3 Consider an arbitrary state of strain with components  $\epsilon_{ij}$  referred to the  $xyz$  coordinate system. Can the components of strain referred to a coordinate system  $x'y'$  that is rotated an angle  $\phi$  about a common  $z$  axis be obtained by simply adding the results of Probs. 2.1 and 2.2?
- 2.4 Write out the general matrix of elastic coefficients for the case where there is a reflection plane normal to the  $z$  axis.

- 2.5☆ Show that an isotropic medium that is both compressible (that is,  $K$  is some finite, non-zero value) and has Poisson's ratio  $\nu = 1/2$  must be a compressible *liquid*. *Hint*: Show that the shear modulus and Young's modulus are both zero, that is,  $\mu = 0$  and  $E = 0$ .  
 Eq. 2.62 shows that when  $\nu = 1/2$ ,  $\mu = E = 0$  and  $K = \lambda$ . Hence, from Eq. 2.57, the material can sustain a state of pressure with  $\sigma_{11} = \sigma_{22} = \sigma_{33} = K(\epsilon_{11} + \epsilon_{22} + \epsilon_{33})$ , but the shear components  $\sigma_{23} = \sigma_{31} = \sigma_{12} = 0$  for any imposed deformation state. It is elastically equivalent to a liquid.
- 2.6 Show that the matrix  $\partial u_i / \partial x_j$  consists of a symmetric matrix (the strain matrix  $\epsilon_{ij}$ ) plus an antisymmetric matrix (the rotation matrix  $\omega_{ij}$ ).
- 2.7☆ For an isotropic substance, derive the stress-strain, strain-displacement, and stress-displacement relations in cylindrical coordinates.  
 The solution is a standard derivation in introductory texts on elasticity. See for example, [https://en.wikipedia.org/wiki/Linear\\_elasticity](https://en.wikipedia.org/wiki/Linear_elasticity)
- 2.8☆ Use symmetry conditions to deduce the number of independent elastic constants for each of the six crystal systems.  
 Eq. 2.26 illustrates the  $6 \times 6$  matrix of elastic constants for a cubic system. Relative to the cubic system, the tetragonal system has a four-fold 3-axis but only two-fold 1 and 2 axes. The four-fold 3-axis means that the 1 and 2 axes can be interchanged so that  $c_{13} = c_{23} \neq c_{12}$  and  $c_{55} = c_{44} \neq c_{66}$ . The complete development for other systems is given in texts on crystal physics such as *Physical Properties of Crystals: Their Representation by Tensors and Matrices* by JF Nye (Oxford University Press, 1985, ISBN-10: 0198511655) or on crystallography.
- 2.9 Use Eq. 2.43 to determine the components of force acting on a surface of area  $A$  with normal parallel to the  $z$  axis. Express your answer in terms of  $A$  and the components  $\sigma_{ij}$  of some arbitrary stress state.



Problem 2.9.

- 2.10☆ Derive expressions for the stress and displacement fields produced by a row of point-force pairs distributed along the axis of a cylinder and acting normal to the axis. Use

these results to determine the stress field of a cylindrical rod forced into a smaller cylindrical hole coaxially positioned in a larger cylinder.

This is a cylindrical analog to the spherical geometry of Sec. 2.7b. Similar to Fig. 2.9, point force pairs are applied to the inner surface of a cylindrical hole at  $r = a$  and the pairs extend along the axis of the cylinder. The outer radius  $R$  is extended to infinity and the outer pressure  $P = 0$ . The only displacement component is  $u_r$  and for an infinite body with a cylindrical hole of radius  $a$  and internal pressure  $p$ ,  $u_r = (p/2\mu) a^2/r$  (e.g., see Timoshenko<sup>‡</sup>). The non-zero cylindrical components of strain are given by  $\epsilon_{rr} = \partial u_r / \partial r$  and  $\epsilon_{\theta\theta} = u_r / r$ . Using the constitutive relations for an isotropic, elastic solid (Eq. 2.57),  $\sigma_{rr} = -pa^2/r^2$  and  $\sigma_{\theta\theta} = pa^2/r^2$ .

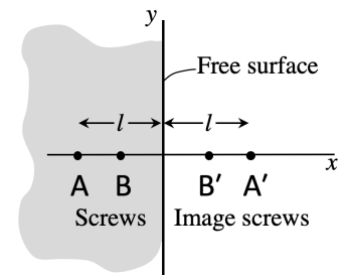
This stress state can be described by the Airy's stress function  $\Psi = -pa^2 \ln r$ , where  $\sigma_{rr} = (1/r)(\partial\Psi/\partial r)$  and  $\sigma_{\theta\theta} = \partial^2\Psi/\partial r^2$  (see Sec. 2.5).

<sup>‡</sup> SP Timoshenko and JN Goodier, *Theory of Elasticity* (3<sup>rd</sup> ed.), McGraw-Hill, 1932, ISBN: 0070701229. Chapter 4: Two-Dimensional Problems in Polar Coordinates.

### CHAPTER 3: THEORY OF STRAIGHT DISLOCATIONS

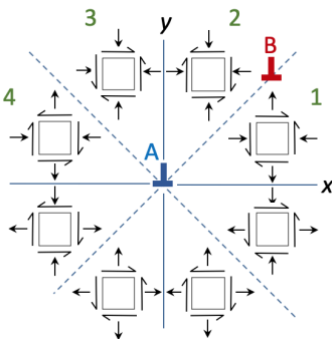
**Description:** These problems provide examples of: the interaction of straight dislocations with other straight dislocations as well free and fixed surfaces; end effects caused by free surfaces; concepts of hollow dislocation cores; and the volume change generated by an edge dislocation.

- 3.1 In Figure 3.6, insert a screw dislocation of the same sign midway between the original screw and the surface. Compute the force exerted on this second screw. Will this force tend to move the inserted dislocation away from or toward the surface?



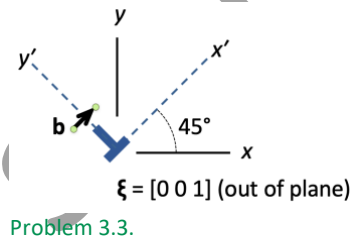
Problem 3.1.

- 3.2 Discuss the interaction between two edge dislocations on parallel glide planes (Figure 3.20). If dislocation A is fixed, find the possible equilibrium positions of dislocation B in glide.



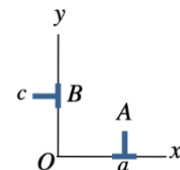
Problem 3.2

- 3.3 Consider an edge dislocation with  $\xi$  along the z axis and  $\mathbf{b}$  inclined at  $45^\circ$  to the x and y axes. An external stress with components  $\sigma_{xx}$ ,  $\sigma_{yy}$ , and  $\sigma_{zz}$  is present. Use Eq. 3.93 to determine the total force per unit length on the dislocation. Discuss the physical significance of the various terms.



- 3.4☆ Consider two straight edge dislocations with mutually orthogonal Burgers vectors of the same magnitude (Figure 3.21). Calculate the energy to move dislocation A from  $x = \infty$  to  $x = a$  within the slip plane. The result shows that dislocations with nonparallel and even orthogonal Burgers vectors interact in general.

The shear stress from dislocation B is given in Eqs. 3.45 but the coordinate system used in those equations is rotated clockwise by  $90^\circ$  relative to the coordinate system in the accompanying figure. The position  $(x, 0)$  in the figure is equivalent to using Eqs. 3.45 with  $x = -c$  and  $y = -x$ . Thus, the shear stress from dislocation B at some position  $(x, 0)$  in the accompanying figure is  $\sigma_{xy}(x) = -[\mu b/2\pi(1-\nu)]c(x^2 - c^2)/(x^2 + c^2)^2$ . The expression shows that  $\sigma_{xy} < 0$  for  $x > c$  and  $\sigma_{xy} > 0$  for  $x < c$  and therefore



Problem 3.4.

dislocation A is attracted to the position  $x = c$ . This can be confirmed by noting the sign of shear stress in the lower left quadrant of the accompanying figure for Prob. 3.2.

The energy (or work) to move dislocation A is calculated by first noting that dislocation B produces a thermodynamic force  $F_x/L = \sigma_{xy}(x)b$  on dislocation A. Therefore, an external force  $(F_x/L)_{\text{ext}} = -\sigma_{xy}(x)b$  must be applied to dislocation A to hold it in equilibrium and the work,  $(F_x/L)_{\text{ext}} dx$ , done by the external force to move A by  $dx$  equals the energy change. The total energy change per unit length of dislocation is therefore

$$\frac{\text{Energy}}{L} = \int_{\infty}^a \left(\frac{F_x}{L}\right)_{\text{ext}} dx = \int_{\infty}^a -\sigma_{xy}b dx = Mc \int_{\infty}^a \frac{x^2}{X^2} dx - Mc \int_{\infty}^a \frac{c^2}{X^2} dx$$

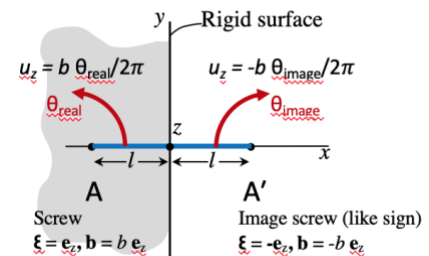
where  $M = \mu b^2/2\pi(1 - \nu)$  and  $X = x^2 + c^2$ . The integral of  $Mcx^2/X^2 dx = Mc[-x/2X + \int dx/2X]$  and that of  $-Mc^3/X^2 dx = -Mc[x/2X + \int dx/2X]$ <sup>‡</sup>. Evaluation of the integral from  $x = R$  to  $x = a$  furnishes

$$\frac{\text{Energy}}{L} = - \left[ \frac{Mcx}{x^2 + c^2} \right]_{x=R}^{x=a} = - \frac{\mu b^2}{2\pi(1 - \nu)} \left[ \frac{ca}{a^2 + c^2} - \frac{cR}{R^2 + c^2} \right]$$

Thus, the energy change when dislocation A is moved from  $x = R$  to  $x = c$  is negative for  $R > a$ , consistent with the attractive Peach-Koehler force over the range  $R > c$ . The second term vanishes in the limit  $R \rightarrow \infty$ .

<sup>‡</sup>From *CRC Standard Mathematical Tables* (21<sup>st</sup> ed.), CRC Press, integrals 111 and 118.

- 3.5 Consider a straight screw dislocation parallel to a rigid surface that cannot deform. Show that the screw is repelled from the surface by a force equivalent to that from an image dislocation of the same sign and magnitude. This result is relevant for dislocations near a surface with a hard oxide layer upon it.



Problem 3.5.

- 3.6★ Suppose that the dislocations in Prob. 3.2 are in a copper crystal. Compute the glide and climb forces on dislocation B if  $x_1 = 7$  nm,  $y_1 = 3$  nm. Compare these forces with those produced by homogeneous external stresses  $\sigma_{xy} = 10^{-3}\mu$ ,  $\sigma_{yy} = 10^{-3}E$ . Note the correction in the question statement (red text).

From Appendix A1, the elastic shear modulus  $\mu = 5.46 \times 10^{10}$  Pa and Poisson's ratio  $\nu = 0.324$ . The Burgers vector magnitude  $b$  is 0.254 nm. The glide and climb forces are given by Eqs. 3.63 and 3.65 with the stress field for an infinite straight edge dislocation in an infinite isotropic body given by Eq. 3.45. The result is  $F_{\text{glide}}/L = F_x/L = 1.9\text{E-4 } \mu \cdot \text{nm}$  and  $F_{\text{climb}}/L = F_y/L = 9.8\text{E-4 } \mu \cdot \text{nm}$ . The homogeneous external stress would produce  $F_x/L = 10^{-3} \mu \cdot 0.254 \text{ nm} = 2.5\text{E-4 } \mu \cdot \text{nm}$  and  $F_y/L = 1\text{E-3 } E \cdot b = 1\text{E-3} \cdot 2 \mu (1 + \nu) \cdot 0.254 \text{ nm} = 6.7\text{E-4 } \mu \cdot \text{nm}$ . Thus, the glide and climb forces produced by the dislocation interaction are comparable to those produced by applied homogeneous stresses  $\sim 10^{-3} \times$  elastic modulus ( $E$  or  $\mu$ ).

- 3.7☆ The results for a screw dislocation in an infinite medium give virtual stresses on the ends of a coaxial finite cylinder enclosing the dislocation (Eq. 3.5). These virtual stresses can be removed by superposition. Consider the counterpart case of an edge dislocation. Show that no long-range stresses exist but that *local* forces do exist on the cylinder end. Estimate the length over which the perturbation caused by these forces extends. *Hint:* Include the stresses from  $\psi_R$ .

From Eq. 3.46, the solution for the infinite medium gives virtual stresses and the nonzero component of interest that generates local forces on the cylinder ends is  $\sigma_{zz} = -C/r$ , where  $C = \mu b \nu (\sin \theta) / [\pi(1 - \nu)]$ . The superposed stress function  $\Psi_R$  (Eq. 3.50) generates  $\sigma_{zz(R)} = -C 2r/R^2$ . The force on the end of the cylinder is obtained by the integration,  $2\pi \int \sigma_{zz} r dr$ , from  $r = 0$  to  $r$  over the end of the cylinder, with the result  $-2\pi Cr$ . Similarly, integration of the contribution from the stress function  $\Psi_R$  gives  $2\pi \int \sigma_{zz(R)} r dr = 2Cr^3/R^2$ . The contributions  $-Cr$  and  $2Cr^3/R^2$  cancel when  $r = R \sqrt{3/2}$ . Thus, end effects from free surfaces are expected to extend a distance  $R \sqrt{3/2}$  from the free surface.

- 3.8☆ Use the results of Exercise 3.5 to predict the equilibrium radius  $r_0$  of a hollow dislocation. Assume the surface energy  $\gamma$  of the hollow tube equals that of a bulk surface. For copper, with  $\gamma = 1.7 \text{ J/m}^2$ , how large a Burgers vector would be required to give a hollow dislocation of radius  $r_0 = 1 \text{ nm}$  (Frank 1951c)?

**MATLAB.** One approach is to compute the energy change,  $\Delta \mathcal{E}$  = the change in elastic strain energy upon introduction of a hollow tube of radius  $r_h$  plus the increase in surface energy upon introduction of a hollow tube.

The reduction in elastic energy upon introduction of the hollow tube is comprised of two terms. The first is  $W/L$  given by Eq. 3.54 with  $R = r_h$ . This quantity,  $[\mu b^2 / (4\pi(1 - \nu))] \ln(r_h/r_0)$ , represents the elastic strain energy that is removed when the material within a tube of radius  $r_h$  is removed from an edge dislocation with core cutoff  $r_0$ , without allowing the new surface at  $r_h$  to relax. The second quantity,  $\mu b^2 / (16(1 - \nu))$ , is the decrease in energy upon relaxation of the new surface to a free surface. This expression is obtained by  $\frac{1}{2} \int \sigma_{rr}(r = r_h) u_r(r = r_h) 2\pi r_h d\theta$ , where  $\sigma_{rr}(r = r_h)$  is given by Eq. 3.46 and  $u_r(r = r_h)$  is given by Eq. 3.53 in Exercise 3.5. The reduction in elastic energy is therefore the sum,  $[\mu b^2 / (4\pi(1 - \nu))] \ln(r_h/r_0) + \mu b^2 / (16(1 - \nu))$ .

The energy change is therefore  $\Delta\mathcal{E} = -[\mu b^2/(4\pi(1-\nu))] \ln(r_h/r_0) - \mu b^2/(16(1-\nu)) + 2\pi r_h \gamma$ , where the last term is the increase in surface energy per unit length of dislocation. The equilibrium condition,  $\partial(\Delta\mathcal{E})/\partial r_h = 0$ , furnishes the result  $r_h = \mu b^2/(8\pi(1-\nu))$ . The Burgers vector magnitude required to obtain  $r_h = 1$  nm is determined by substituting  $\mu = 5.46\text{E}10$  Pa,  $\nu = 0.324$ , and  $\gamma = 1.7$  J/m<sup>2</sup> for copper. The result is  $b = 0.56$  nm.

This solution adopts the standard assumption that any hollow dislocation has right-circular cylindrical symmetry. However, the core for edges is likely to deviate from that configuration ( see J. P. Hirth, *Acta Materialia*, 47, 1999).

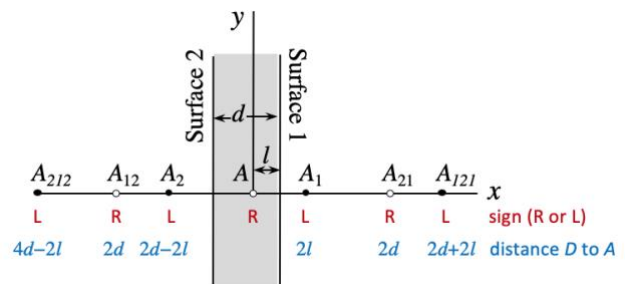
- 3.9 Consider a right-handed screw dislocation parallel to the surfaces of an infinite plate (Figure 3.22). The image dislocation  $B$  satisfies the boundary condition on surface 1 but leaves a residual stress on surface 2. Thus, an additional image  $E$  is required, which in turn requires an image  $F$ , etc. A similar set is associated with image  $C$ . The result is an infinite set of image dislocations. Show that the sum of all the image stresses acting at the origin on dislocation  $A$  is

$$\sigma_{yz} = -\frac{\mu b}{4\pi d} \sum_{n=-\infty}^{\infty} \frac{1}{n - (1/d)} = \frac{\mu b}{4\pi d} \sum_{n=-\infty}^{\infty} \frac{1}{n + (1/d)}$$

The solution to this sum is (Morse and Feshbach 1951: 383)

$$\sigma_{yz} = -\frac{\mu b}{4d} \cot \pi l / d$$

Note that the set of right-handed image dislocations is symmetric about the origin, so that  $\sigma_{yz}$  at the origin is produced completely by the left-handed set.



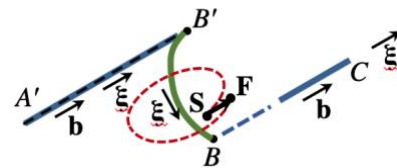
Problem 3.9.

- 3.10☆ Show that the external volume change for an edge dislocation located on the axis of a right-circular cylinder is zero. This result is true for a dislocation in a finite body of any shape, since one can always create the dislocation by applying equal and opposite tractions to opposite sides of a glide plane cut. This can be demonstrated from Eq. 2.93. Similar to the derivation leading up to Eq. 2.93, the volume change per unit length of dislocation is  $\int r u_r d\theta$ . The displacement  $u_r$  for an edge dislocation in an infinite medium is given by Eq. 3.49. The only significant term is the first which integrates to zero over the domain from  $\theta = 0$  to  $2\pi$ . The second is also zero for a similar reason. The third integral involves  $\int \theta \cos \theta d\theta = \cos \theta + \theta \sin \theta$  using integration by parts. Thus, the third integral is also zero. The zero change of volume is exact. This exact nature is related to the work of Eshelby and Rice, discussed in Sec. 3.8.

#### CHAPTER 4: THEORY OF CURVED DISLOCATIONS

**Description:** These problems offer practice in identifying the vacancy/interstitial nature of loops formed by dislocation motion, the transport of matter associated with dislocation motion, and the use of Eqs. 4.30 and 4.20 to compute the stress and displacement fields of curved dislocations.

- 4.1 Consider the pure screw dislocation lying along  $ABC$  in Figure 4.7. A screw with a loop results if  $AB$  is moved conservatively through positions  $A'B'$ ,  $A''B''$ , etc., while  $BC$  is held fixed. Is the loop a vacancy or an interstitial loop?

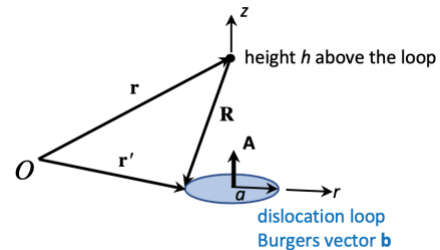


Problem 4.1.

- 4.2 The formation of the loop in Prob. 4.1 requires material transport. Where is the source or sink for this matter? *Hint:* Consider that the screw emerges normal to a free surface at  $A$  and study the configuration at  $A$  as the loop is formed.
- 4.3 Use Eq. 4.30 to derive the stress field for a pure screw dislocation in an infinite medium.

4.4 ☆ Demonstrate that the displacements  $\mathbf{u}(\mathbf{r})$  given by Eq. 4.20 change discontinuously by  $\Delta\mathbf{u} = \pm\mathbf{b}$  if the point  $\mathbf{r}$  is intersected by the surface.

The first term of Eq. 4.20 is  $-\mathbf{b}\Omega/4\pi$  where the solid angle  $\Omega$  is defined in Eq. 4.21. Drawing on the development in Fig. 4.4 where the vectors  $\mathbf{r}$ ,  $\mathbf{r}'$ , and  $\mathbf{R}$  are defined, consider a point with position vector  $\mathbf{r}$  located a distance  $h$  above a dislocation loop defined by area  $A$  and radius  $a$  as shown in the accompanying figure. Then  $R = (r^2 + h^2)^{1/2}$ ,  $dA = r dr d\theta$ , and  $\mathbf{R} \cdot d\mathbf{A} = -h 2\pi r dr$ . The solid angle expression from Eq. 4.21 is then



Problem 4.4.

$$\Omega = -2\pi \int_0^a \frac{-h r dr}{(r^2 + h^2)^{3/2}} = \left. \frac{-2\pi h}{(r^2 + h^2)^{1/2}} \right|_0^a = \left[ \frac{-2\pi h}{(a^2 + h^2)^{1/2}} + 1 \right] = 2\pi \text{ as } h \rightarrow 0^+$$

Substitution of  $\Omega(0^+) = 2\pi$  into the first term of Eq. 4.20 gives  $\mathbf{u}(h = 0^+) = -\mathbf{b}/2$ . A similar calculation gives  $\mathbf{u}(h = 0^-) = \mathbf{b}/2$  for a point positioned just below the dislocation loop. The change in sign occurs because  $\mathbf{R} \cdot d\mathbf{A}$  changes sign since  $\mathbf{R}$  points upward for  $h = 0^-$  but points downward for  $h = 0^+$ . The other terms in Eq. 4.20 are not discontinuous from  $0^+$  to  $0^-$  and therefore the jump in displacement is  $\Delta\mathbf{u} = \mathbf{u}(h = 0^+) - \mathbf{u}(h = 0^-) = -\mathbf{b}$ . Physical examples of a jump are shown in Figs. 1.19 and 1.23.

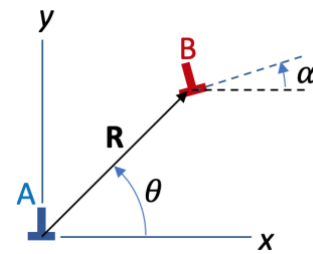
- 4.5★ Show that the displacements given by Eq. 4.20 are dependent only on the configuration of the dislocation *line* that forms the loop and not on the shape of the surface *A*, provided surface *A* is not intersected in the manner of Prob. 4.4.

The integrals in Eq. 4.20 can be converted to line integrals so that the results are independent of the shape of the (cut) surface and only dependent on the configuration of the dislocation. Recall the result for Prob. 1.7.

## CHAPTER 5: APPLICATIONS TO DISLOCATION INTERACTIONS

**Description:** These problems provide examples of interaction energies and forces between loops and parallel and nonparallel straight dislocations, as well as stress fields of infinitesimal loops and angular dislocations.

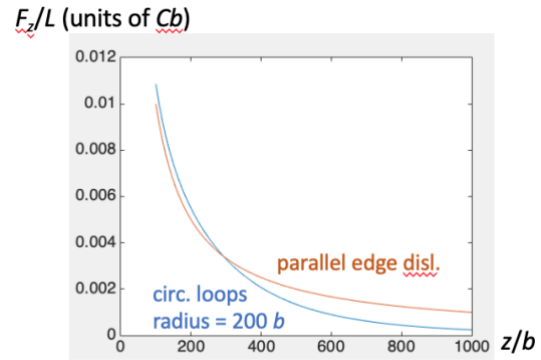
- 5.1 Consider two parallel edge dislocations *A* and *B* with Burgers vectors inclined at an angle  $\alpha$ . Dislocation *A* is constrained to remain at the origin of the coordinate system and both dislocations are constrained to remain parallel.



Problem 5.1.

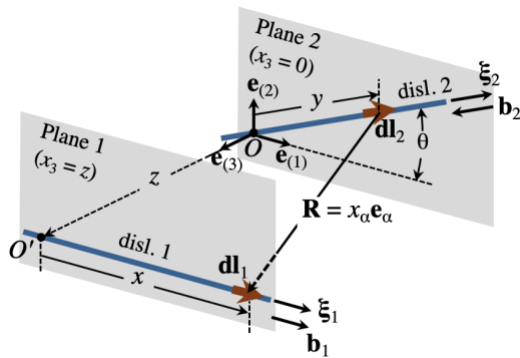
- a. Explicitly express the interaction force on *B* as a function of  $R$ ,  $\theta$ , and  $\alpha$ .
  - b. Is there an equilibrium position for dislocation *B*? If so, where?
  - c. For constant  $R$ , show that  $F_\theta$  vanishes when  $\theta = \alpha/2$ .
- 5.2★ Graphically compare the interaction force per unit length for two cases: (a) the two coaxial dislocation loops of Figure 5.2 as a function of  $z$  for the case  $a = c = 200b$ ; (b) two parallel edge dislocations in the same glide plane as a function of their separation in the glide plane. In which case does the interaction force decrease more rapidly with increasing separation? Why?

**MATLAB.** Eq. 5.26 provides the interaction energy  $W_{12}$  for a pair of circular dislocation loops as shown in Fig. 5.2, with radius  $a$  and Burgers vector  $\mathbf{b}_1 = \mathbf{b}_2 = b\mathbf{e}_z$  for both loops. The interaction energy per unit length is therefore  $W_{12}/L = C k(K - E)$ , where  $k^2 = 4/(4 + a^2/z^2)$  and  $K(k)$  and  $E(k)$  are complete elliptic integrals of the first and second kind, respectively, and  $C = \mu b^2/2\pi(1 - \nu)$ . The interaction force in the  $z$  direction per unit length of loop is  $F_z/L = -\partial(W_{12}/L)/\partial z$ . For comparison, Eq. 5.18 shows that two infinitely long edge dislocations with  $\mathbf{b}_1 = \mathbf{b}_2 = b\mathbf{e}_z$  separated by  $z$  have an interaction force  $F_z/L = C/R$ . The accompanying figure shows  $F_z/L$  for two circular loops of radius  $a = 200b$  and for the two infinitely long edge dislocations. The loop interaction falls off more rapidly because the field of the loop is limited approximately to a sphere of radius  $a$  according to St. Venant's principle.



Problem 5.2.

- 5.3 ☆ Consider two perpendicular screw dislocations and determine the local interaction force as a function of position on the dislocation line. Assume that one screw is right-handed and the other left-handed and that they are forced together by uniform external stresses. Qualitatively deduce the dislocation configuration when the interaction forces balance those caused by the applied stresses.



Problem 5.3.

Eq. 5.48 defines the force function  $\delta\mathbf{F} = \delta\mathbf{F}(y_2, x) - \delta\mathbf{F}(y_1, x)$ , where  $\delta\mathbf{F}$  is the force exerted on dislocation segment  $d\mathbf{l}_1$  at coordinate  $x$  by dislocation 2 that spans from coordinates  $y_1$  to  $y_2$  along  $\xi_2$ . The coordinates  $x$  and  $y$  are defined in Figure 5.4, which is reproduced here for convenience. The dislocations are oppositely signed, perpendicular screws so  $\theta = \pi/2$  in the figure. Dislocation 1 is chosen to be right-handed, so that  $\mathbf{b}_1 \cdot \xi_1 = b$ , and dislocation 2 is chosen to

be left-handed, so that  $\mathbf{b}_2 = -b\xi_2$  and  $\mathbf{b}_2 \cdot \xi_2 = -b$ .

Eq. 5.50 is used to determine  $\delta\mathbf{F}(y, x)$ . The first term, Eq. 5.50a, is the only nonzero contribution because the dot and cross products in terms  $b, c,$  and  $d$  are zero. Eq. 5.50a is rewritten as Eq. 5.55a (p. 121, top). In that expression, only the first term survives since  $\theta = \pi/2$  and  $b_{1e} = b_{2e} = 0$ . Therefore,  $\delta\mathbf{F}(y, x) = -(\mu b^2/4\pi)(z/\rho R) d\mathbf{l}_1 \mathbf{e}_3$ , where  $\rho, R,$  and  $h_3$  are defined near the top of p. 122. (Note: the same result for  $\delta\mathbf{F}(y, x)$  is obtained from the first term of the original Eq. 5.50a, where  $\mathbf{b}_2 \times \mathbf{b}_1 = -b^2 \mathbf{e}_3, \nabla(\nabla^2 R) =$

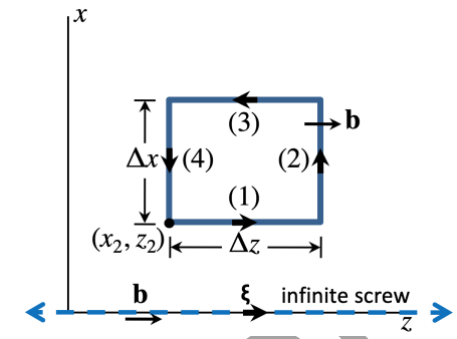
$\nabla(2/R) = (\partial/\partial x)(2/R^2)\mathbf{e}_1 + (\partial/\partial y)(2/R)\mathbf{e}_2 + (\partial/\partial z)(2/R)\mathbf{e}_3$ ,  $d\mathbf{l}_1 \times d\mathbf{l}_2 = dl_1 \xi_1 \times dy \xi_2 = dl_1 dy \mathbf{e}_3$ , and  $\int(\partial/\partial z)(1/R) dy = z/\rho R$ .)

Thus,  $\delta\mathbf{F} = \delta\mathbf{F}(y_2, x) - \delta\mathbf{F}(y_1, x)$ , where  $y_1 = -\infty$  and  $y_2 = +\infty$  are chosen to model an infinitely long dislocation 2.  $\delta\mathbf{F}(+\infty, x) = 0$  and  $\delta\mathbf{F}(-\infty, x) = -(\mu b^2/4\pi)(z/[(y_1 + R)R]) dl_1 \mathbf{e}_3$  as  $y_1 \rightarrow -\infty$ . The limit is evaluated by noting that for  $x$  and  $z \ll y_1$ , a Taylor's series can be used to write  $\rho(x, y_1, z) \equiv y_1 + R = \rho(0, y_1, 0) + (\partial\rho/\partial x)_{(0,y,0)} x + (\partial\rho/\partial z)_{(0,y,0)} z + (\partial^2\rho/\partial x^2)_{(0,y,0)} x^2/2 + (\partial^2\rho/\partial z^2)_{(0,y,0)} z^2/2 + \text{higher order terms}$ .  $\rho(0, y_1, 0) = (\partial\rho/\partial x)_{(0,y,0)} = (\partial\rho/\partial z)_{(0,y,0)} = 0$  and  $(\partial^2\rho/\partial x^2)_{(0,y,0)} = (\partial^2\rho/\partial z^2)_{(0,y,0)} = 1/R$ . Therefore,  $\delta\mathbf{F}(-\infty, x) = -[\mu b^2 z / (8\pi(x^2 + z^2))] dl_1 \mathbf{e}_3$  and  $\delta\mathbf{F} = \mu b^2 z / (8\pi(x^2 + z^2)) dl_1 \mathbf{e}_3$ . One can confirm that  $\delta\mathbf{F}$  has dimensions of force and that it acts along  $\mathbf{e}_3$ , consistent with segment  $dl_1$  being repelled the oppositely signed, perpendicular, screw dislocation (2).  $\delta\mathbf{F}$  is largest in magnitude at  $x = 0$ , which corresponds to the minimum perpendicular distance between  $dl_1$  and dislocation 2.

The interaction force is balanced by those from a uniform applied stress when  $\delta\mathbf{F} - \sigma b dl_1 \mathbf{e}_3 = 0$ . Therefore,  $z$  is a maximum at  $x = 0$ , where the repulsive force is largest. Figure 22.2 shows an approximate sketch of the configuration. The exact equilibrium configuration must include the additional force exerted on  $dl_1$  by other segments along dislocation 1.

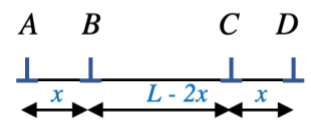
- 5.4 Solve for the local interaction forces between a screw dislocation and a perpendicular edge dislocation whose Burgers vector is parallel to the line of closest approach between the two. Show that the interaction forces on one dislocation are perpendicular to the interaction forces on the other, so that there is no equal and opposite action and reaction. Discuss this apparent violation of Newton's law.

- 5.5 Compute the maximum local interaction force between the loop of Figure 5.12 and a straight screw dislocation lying in the same glide plane and with its Burgers vector parallel to the  $z$  axis.



Problem 5.5.

- 5.6 ☆ Compute the five stress components other than  $\sigma_{yz}$  (Eq. 5.70) for the angular dislocation.  
 The geometry is shown in Figure 5.10. The results for the other components are given by Yoffe EH (1961) *Phil. Mag.* 6: 1147.
- 5.7 ☆ Compute the six general stress components around the infinitesimal glide dislocation loop in Figure 5.12.  
 The results are given by Kroupa F (1962a) *Czech, J. Phys.* 12B: 191.
- 5.8 Consider four parallel edge dislocations lying on the same glide plane. There is no external stress but they are blocked at both ends of an interval  $L$  by barriers that exert short-range repulsive forces, extending over atomic dimensions only. Determine the equilibrium configuration of the array if the dislocations are constrained not to climb.



Problem 5.8.

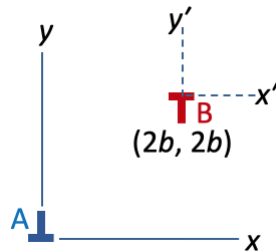
- 5.9 ☆ Compute the long-range stress field around a dislocation dipole consisting of two parallel edge dislocations with equal and opposite Burgers vectors. Assume they are in

glide equilibrium with glide planes that are separated by a distance  $2b$ . *Hint:* Use the interaction force on an element as a “test probe” for the stress.

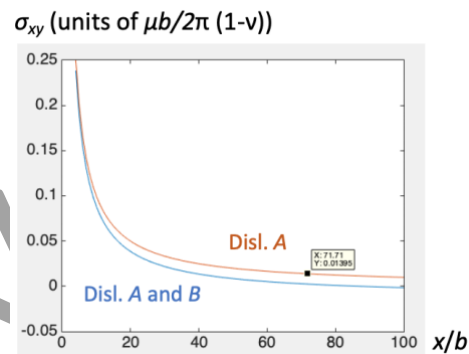
**MATLAB.** The relevant geometry for the two dislocations,  $A$  and  $B$ , is shown in the accompanying Figure 1 (below). Consider Eq. 3.45 for the stress field from dislocation  $A$ . The superposition of  $\sigma_{xy}$  from  $A$  and  $B$  gives the following,

$$\sigma_{xy} = \frac{x(x^2 - y^2)}{(x^2 + y^2)^2} - \frac{x'(x'^2 - y'^2)}{(x'^2 + y'^2)^2}$$

where  $x' = x - 2b$  and  $y' = y - 2b$ . The accompanying Figure 2 shows a plot of  $\sigma_{xy}$  as a function of  $x/b$ . Also shown is  $\sigma_{xy}$  from only  $A$ ; it varies as  $1/x$ . The result shows that  $\sigma_{xy}$  from the  $A$ - $B$  dipole falls off faster than that from  $A$  alone, thereby demonstrating St. Venant's principle.



Problem 5.9, Figure 1.



Problem 5.9, Figure 2.

5.10☆ Discuss the role of grain boundaries as sources of image stresses in real crystals.

In the isotropic approximation, grain boundaries do not produce image stresses. For anisotropic analyses, there will be an elastic mismatch at the grain boundary except for special coincidence or twin boundaries. Hence, general grain boundaries will generate image forces and contribute to interactions between dislocations. While not exact, the relative importance of image forces roughly scales with the anisotropy ratio, values of which are listed in Appendix A.

## CHAPTER 6: APPLICATIONS TO SELF ENERGIES

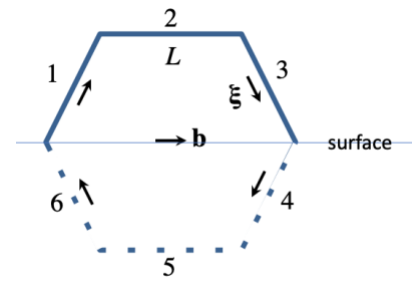
**Description:** These problems provide examples of the energy of various polygonal dislocations, including edge and screw bow outs, loops at free surfaces, zig-zag formation along straight dislocations, as well as triangular, square, hexagonal, and circular loops.

6.1☆ Compute the energy of a semi-hexagonal dislocation loop lying normal to and terminating at a free surface. The Burgers vector is parallel to the free surface. Use a simple image construction. Compare the results with those of Eqs. 6.72 and 6.73.

The accompanying Figure 1 shows the geometry of the semi-hexagonal loop (solid lines) and the image (dashed lines). The sense of the loop is continuous (clockwise) and  $\mathbf{b}$  is the same for all segments 1-6. Thus, segments 2 and 5 are oppositely signed

segments, consistent with a free-surface image construction. Segment 6 is an image of segment 1, and 4 is an image of 3. This is evident if the sense (and Burgers vector) of 6 and 4 are reversed.

Eq. 6.5 can be used for the sum of the self and interaction energies and compared to the energy change for a large bow-out that forms on a screw dislocation (Eq. 6.72) or edge dislocation (Eq. 6.73):



Problem 6.1, Figure 1.

$$\frac{W}{C} = 3(2 - \nu) \left[ \ln \frac{L}{\rho} - 0.84 \right] = 5 \ln \frac{L}{\rho} - 4.2 \text{ for } \nu = \frac{1}{3} \text{ (hexagonal loop, Fig. 6.7)}$$

$$\frac{\Delta W}{C} = \left( 1 + \frac{\nu}{2} \right) \ln \frac{L}{\rho} - 0.04\nu - 2.05 = 1.2 \ln \frac{L}{\rho} - 2.1 \text{ for } \nu = \frac{1}{3} \text{ (screw bow out, Fig. 6.9)}$$

$$\frac{\Delta W}{C} = \left( 1 - \frac{3\nu}{2} \right) \ln \frac{L}{\rho} + 2\nu - 2.05 = 0.5 \ln \frac{L}{\rho} - 1.4 \text{ for } \nu = \frac{1}{3} \text{ (edge bow out, Fig. 6.9)}$$

$$\text{where } C = \frac{\mu b^2 L}{4\pi(1 - \nu)}$$

A bow-out on an edge dislocation has the smallest logarithmic coefficient, followed by a bow out on a screw. A bow out at a free surface (hexagonal loop) has the largest logarithmic coefficient because the strong attraction between segments 1 and 5 is larger than the weak interaction of segment CD with AB and EF (Fig. 6.9). Thus, a semi-hexagonal bow out on a screw or edge dislocation is more likely than one at a free surface. This calculation does not include the additional creation (or removal) of a ledge at the surface for the case of a bow out at a surface.

**Extra Material:** Calculation of energies of loops can be tedious and thus the terms for the energy of a hexagonal loop are provided.

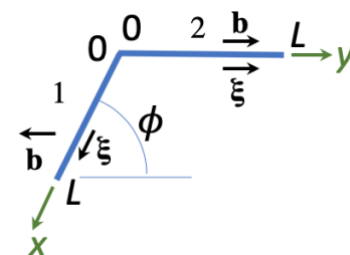
For two coplanar, non-parallel segments, Eq. 6.41 can be used to calculate the interaction energy. For the bow out configurations considered here,  $\mathbf{b}$  is in the  $(x_1 - x_2)$  plane of the segments and thus only the term with  $I(x_\alpha, y_\beta)$  contributes. Also,  $\mathbf{b}$  is common to all segments so that the  $\mathbf{b}_1 \times \mathbf{b}_2$  term vanishes. For this case, the interaction energy between segments  $p$  and  $q$  takes the form

$$W_{pq} = \frac{\mu b^2}{4\pi} \left( C_s + \frac{C_e}{1 - \nu} \right) I(x_\alpha, y_\beta)$$

The results below list the values of  $C_s$ ,  $C_e$ , and  $I(x_\alpha, y_\beta)$  for interaction between the segments in the hexagonal geometry in the accompanying Figure 1 (above).

### Segments 1 & 2

In this case, the sense and Burgers vector are both changed in sign for segment 1 and Eq. 6.41 is applied.



Problem 6.1, Figure 2. Segments 1&2.

$$C_s = \cos \phi$$

$$C_e = 0$$

$$I(x_\alpha, y_\beta) = I(L, L) + I(0, 0) - I(L, 0) - I(0, L) = 2L \ln [(1 + \cos \phi + 2 \cos \phi/2)/(1 + \cos \phi)],$$

where the numerator of the ln term arises from  $I(L, L)$  and the denominator from  $-I(L, 0) - I(0, L)$ .  $I(0, 0) = 0$ .

### Segments 1 & 3

Similar to the previous case, the sense and Burgers vector are both changed in sign for segment 1 and Eq. 6.41 is applied.

$$C_s = \cos^2 \phi$$

$$C_e = -\sin^2 \phi$$

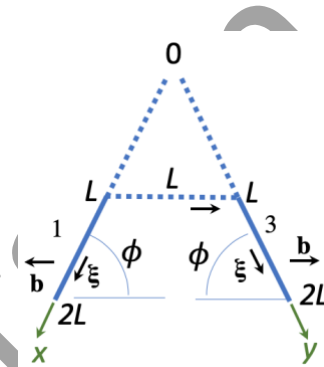
$$I(x_\alpha, y_\beta) = I(2L, 2L) + I(L, L) - I(2L, L) - I(L, 2L) \text{ where}$$

$$I(2L, 2L) = 4L \ln(2 + \cos 2\phi)$$

$$I(L, L) = 2L \ln(2 + \cos 2\phi)$$

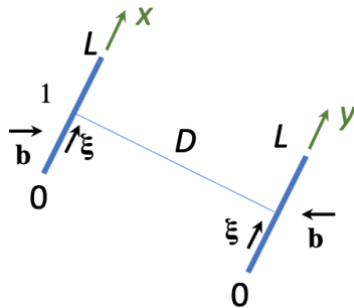
$$I(2L, L) = I(L, 2L) = 2L \ln(\cos \phi/2 + 1/2 + \cos 2\phi) +$$

$$L \ln(2 \cos \phi/2 + 2 + \cos 2\phi)$$



Problem 6.1, Figure 3. Segments 1&3.

### Segments 1 & 4



Problem 6.1, Figure 4. Segments 1&4.

In this case, the segments are parallel and the sense and Burgers vector for segment 4 are reversed.

Application of Eq. 6.45 gives

$$C_s = -\cos^2 \phi$$

$$C_e = -\sin^2 \phi$$

$$I(x_\alpha, y_\beta) = I(L, L) + I(0, 0) - I(L, 0) - I(0, L) \text{ where}$$

$$I(L, L) = I(0, 0) = D$$

$$I(L, 0) = I(0, L) = R + (L/2) \ln[(R - L)/(R + L)], \text{ where } R = (D^2 + L^2)^{1/2}$$

### Segments 1 & 5

In this case, the sense and Burgers vector for segment 5 are reversed and Eq. 6.41 gives

$$C_s = -\cos \phi$$

$$C_e = 0$$

$$I(x_\alpha, y_\beta) = \text{same as for segments 1 \& 3}$$

### Segments 1 & 6

In this case, the sense and Burgers vector for segment 6 are reversed and Eq. 6.41 gives

$$C_s = -\cos^2\phi$$

$$C_e = \sin^2\phi$$

$l(x_\alpha, y_\beta)$  = same as for segments 1 & 2

### Segments 2 & 5

In this case, the segments are parallel and the sense and Burgers vector for segment 5 are reversed. Application of Eq. 6.45 gives

$$C_s = -1$$

$$C_e = 0$$

$l(x_\alpha, y_\beta)$  = same as for 1 & 4.

The energy of the hexagonal loop is then expressed as:

$$W_{\text{hexagon}} = 2W_{s(\text{screw})} + 4W_{s(\text{mixed})} + 4W_{12} + 2W_{13} + 2W_{14} + 4W_{15} + 2W_{16} + W_{25}$$

where

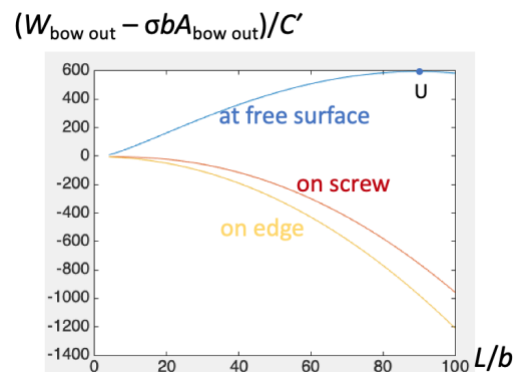
$$W_{s(\text{screw})} = \frac{\mu b^2}{4\pi} L \ln \frac{L}{e\rho}, W_{s(\text{mixed})} = \frac{\mu b^2}{4\pi} \left( \cos^2\phi + \frac{\sin^2\phi}{1-\nu} \right) L \ln \frac{L}{e\rho},$$

where  $\phi$  is the angle subtended by the Burgers vector and dislocation sense. The multiplying factors for each of the  $W_{ij}$  terms above occur because within the loop,

- $W_{12} = W_{32} = W_{45} = W_{56}$  (mixed-screw 1<sup>st</sup> nearest neighbors)
- $W_{13} = W_{46}$  (mixed-mixed 2<sup>nd</sup> nearest neighbors)
- $W_{14} = W_{36}$  (parallel mixed-mixed)
- $W_{15} = W_{24} = W_{26} = W_{35}$  (mixed-screw 2<sup>nd</sup> nearest neighbors)
- $W_{16} = W_{34}$  (mixed-mixed 1<sup>st</sup> nearest neighbors)

6.2☆ Suppose that each loop in Prob. 6.1 assumes an unstable equilibrium configuration under the same force  $\sigma b$ . Which case will have a larger equilibrium value  $L$ ?

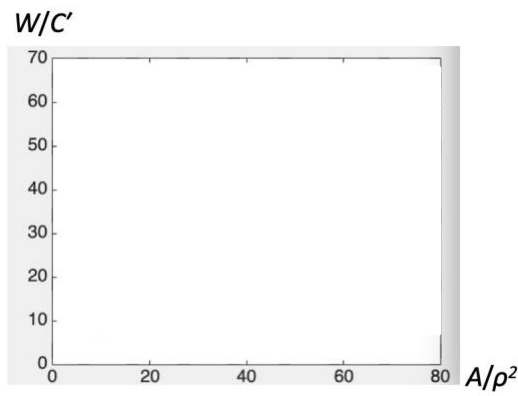
**MATLAB.** The energies of the bow out configurations in Prob. 6.1 were ranked with the coefficient of the logarithmic term being largest for the bow out from a free surface and smallest for a bow out on an edge dislocation. The effect of a uniform applied shear stress  $\sigma$  acting on the slip plane in the direction of  $\mathbf{b}$  is to generate a Peach-Koehler force,  $\sigma b$ , that does work,  $\sigma b A_{\text{bow out}}$ , where the area slipped by the bow out is  $A_{\text{bow out}} = 1.3 L^2$ .



Problem 6.2.

The energy to create the bow outs is provided by the  $W/C$  and  $\Delta W/C$  expressions in the solution to Prob. 6.1. The accompanying Figure shows a plot of  $(W - \sigma b 1.3 L^2)/C'$  as a function of  $L/b$ , for  $\sigma b/C = 0.1$ , where  $C' = CL = \mu b^2/(4\pi(1-\nu))$ . The bow out at a free surface has the largest unstable equilibrium value (shown by the location U). This is logical because the bow out at a free surface has the largest prelogarithmic factor among the cases considered. At this value of stress, the “on screw” and “on edge” cases have sufficient stress to expand over the entire range of  $L/b$  shown.

- 6.3 Determine the energy of regular polygons with 3, 4, 8, 12, and  $n$  sides, assuming equal area loops. Compare the results with those given for the circle and the hexagon. Take  $\mathbf{b}$  normal to the plane of the loop in each case.



Problem 6.3.

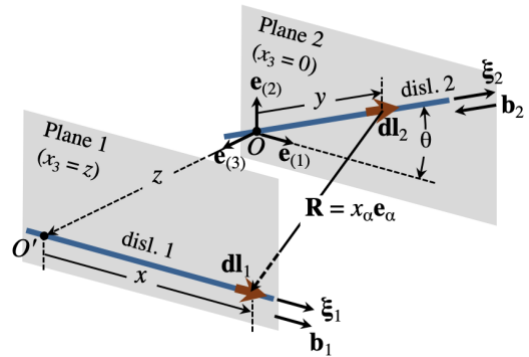
- 6.4★ Calculate the energy of the square loop of Figure 6.12 as a function of the angle  $\phi$ .

The energy increases with increasing  $\phi$  until  $\phi = \pi/2$ . This occurs because the two initially-screw segments develop an increasing edge component until they become pure edge at  $\phi = \pi/2$ .

- 6.5☆ Compute the interaction energy between two perpendicular screw dislocations. Differentiate this energy with respect to the separation distance between the two and show that the resulting force agrees with that of Exercise 5.5.

Eq. 6.33 is used with  $\theta = \pi/2$  in the accompanying figure. Dislocation 1 is chosen to be right-handed, so that  $\mathbf{b}_1 \cdot \boldsymbol{\xi}_1 = b$ , and dislocation 2 is chosen to be left-handed, so that  $\mathbf{b}_2 = -b\boldsymbol{\xi}_2$  and  $\mathbf{b}_2 \cdot \boldsymbol{\xi}_2 = -b$ . Thus, only the first term in Eq. 6.33 is nonzero and since  $\boldsymbol{\xi}_1 \times \boldsymbol{\xi}_2 = \mathbf{e}_3$  and  $\mathbf{b}_2 \times \mathbf{b}_1 = -b^2 \mathbf{e}_3$ ,  $W_{12} = (\mu b^2/4\pi)I(x_\alpha, y_\beta)$ .

$I(x_\alpha, y_\beta)$  is defined by Eq. 6.27 where  $x_2$  and  $y_2 \rightarrow \infty$  and  $x_1$  and  $y_1 \rightarrow -\infty$  and  $I(x, y)$  is defined in Eq. 6.36 and equals  $\frac{1}{2}(x + y) \ln[z^2/((R - x)(R - y))]$ . This can be differentiated so that  $F_z = -\partial W_{12} / \partial z$ . The process is tedious.



Problem 6.5.

An alternative approach is to use the result of Prob. 5.3 where the force exerted by dislocation 2 on an infinitesimal segment  $d\mathbf{l}_1$  is  $\delta\mathbf{F} = [\mu b^2 z / (8\pi(x^2 + z^2))] d\mathbf{l}_1 \mathbf{e}_3$ . Integration with respect to  $x$  gives  $F_z = -(\mu b^2 / 8\pi) \tan^{-1}(x/z)$ , evaluated from  $x = -\infty$  to  $x = +\infty$ . The result is  $F_z = -\mu b^2 / 8$ , signifying an attractive force (See. Fig. 22.2). The result is independent of the separation distance  $z$ , for infinitely long dislocations and dependent on  $z$  if the length of dislocation 1 is finite.

- 6.6☆ Under what conditions could a straight dislocation line spontaneously break up into a zigzag dislocation line? *Hint:* The problem is analogous to that of breaking up a flat surface into a hill-and-valley structure (Herring 1949). In the isotropic approximation, can any type of dislocation break up in this manner?

One can think of the small bow out configuration (Fig. 6.8) as an incipient zig-zag. The zig-zag is stable if the energy per unit length of the pair of segments  $AC$  and  $CB$  is sufficiently less than that of the initial segment  $AB$  that it offsets the increase in line length. That is, a torque acts on the incipient segments and leads to a zig-zag shape. The torque associated with the screw-edge character in the isotropic elastic approximation is insufficient to cause the zig-zag instability for pure crystals. Selective solute adsorption to the dislocation could cause the instability. However, for pure crystals in the anisotropic case, the variation in energy with screw-edge character can be greater and it can and does cause the instability.

## CHAPTER 7: DISLOCATIONS AT HIGH VELOCITIES

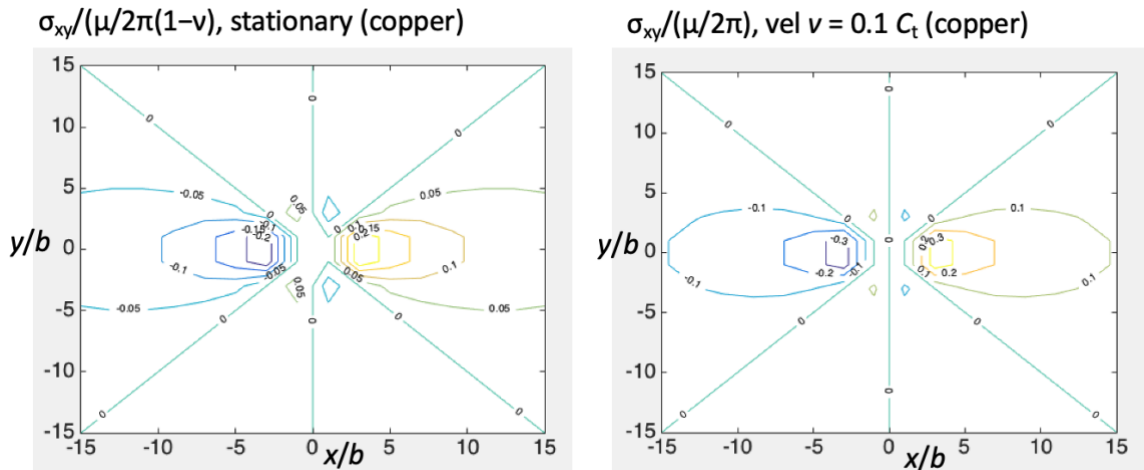
**Description:** These problems consider the effects of dislocation motion on cross slip and interaction between dislocations, the time for dislocations to achieve a specified velocity from a stationary position upon application of a uniform stress, fundamental frequencies of vibration of segments and dampening, and contributions of kinetic energy to ledge formation at surfaces.

- 7.1 ☆ Consider a screw dislocation moving at a velocity  $v = C_t/10$ , parallel to a free surface and a distance  $l$  below it. Compared to a static screw in the same position, is the moving dislocation more or less likely to cross slip out of the crystal because of the image interaction?

Less likely. Although the image force exerted on the screw is of magnitude  $\mu b^2/(4\pi L\gamma)$  and increases with increasing velocity (see Eq. 7.10 for  $\gamma$ ), inertia keeps the dislocation moving in the same direction and thus cross slip is less likely.

- 7.2 Consider a screw dislocation moving parallel to the surface of a semi-infinite slab and a distance  $l$  below the surface. If the applied stress  $\sigma = 10^{-3}\mu$ , how long will it take for the dislocation to reach a velocity  $0.9 C_t$  starting at rest? How far has it moved? Assume quasi-uniform motion and ignore all friction.

- 7.3 ☆ Plot the distribution of shear stress  $\sigma_{xy}$  around an edge moving at a velocity  $v = C_t/10$  and compare the result with the static case. Use the physical parameters for copper, with the elastic constants given in Appendix 1. How will two like-sign edge dislocations interact if they are moving uniformly on the same glide plane? On parallel glide planes?



Problem 7.3.

**MATLAB.** The accompanying figure shows the stress fields for the static (Eq. 3.45) and moving (Eq. 7.24 with the sign of  $b$  changed and  $\nu = 0.1 C_t$ ) cases. The  $\pm 45^\circ$  contours in the stationary case are slightly shifted to be less than  $\pm 45^\circ$  for the moving case, consistent with the depiction in Fig. 7.5. The decrease in angle is almost imperceptible in the figure but it becomes more noticeable at larger velocity. The moving dislocation has larger values of shear stress along the  $x$ -axis and smaller values along the  $y$ -axis, compared to the stationary case. Therefore, like-sign dislocations on the same glide plane have a larger repulsion force at  $\nu = 0.1 C_t$ . For the two dislocations separated in the  $y$ -direction, the angular range over which the dislocations attract increases with  $\nu$  and covers the entire range of positions at  $\nu_R$ . This has consequences for the Zener model of a shock front. The restoring force to keep the two dislocations vertically aligned increases with increasing  $\nu$  up to  $\nu_R$ .

- 7.4 Consider a screw segment of length  $L$  that is pinned at the ends. If the segment is visualized as a string with a line tension  $S$  and effective mass per unit length  $m^*$ , what is the basic frequency of vibration? Determine the appropriate effective mass.

- 7.5☆ Assume that the radiation per unit length from the vibrating string in Prob. 7.4 is given approximately by Eq. 7.49. How rapidly does the fundamental vibration dampen out? Ignore all other dissipative mechanisms.

A simple approximation for the time to dampen out the fundamental frequency is

$$t = \frac{W_0/L}{\dot{W}/L} = \frac{4}{\pi^4} \ln(R/r_0) \frac{L^3}{X^2 C_t}$$

where expressions for  $W_0/L$  and  $\dot{W}/L$  are obtained from Eqs. 3.13 and 7.49 and  $\Omega = C_t/2L$ . Using  $C_t = 2.47\text{E}3$  m/s (Eq. 7.3) for copper,  $R/r_0 = 200$ , and vibration amplitude  $X = 2b$ , then the time to dampen out the fundamental vibration is  $t = 5.6\text{E}-13$  s.

- 7.6☆ Assume that the effective mass of an edge dislocation is given by Eq. 7.64 with an outer cutoff radius  $R \sim 10^4 b$ . Determine the kinetic energy of an edge dislocation in copper moving at a velocity  $v = C_t/10$ . Suppose that the dislocation approaches a grain boundary. Determine whether the kinetic energy is sufficient to supply the surface energy of the step formed on the grain boundary when the edge intersects it. Assume the surface energy of the grain boundary step is  $\gamma = 0.6$  J/m<sup>2</sup>. Neglect image forces.

The condition for the kinetic energy to supply the surface energy of the step is

$$\frac{1}{2} m^* v^2 > \gamma b$$

For copper,  $C_t = 2.47\text{E}3$  m/s (see Prob. 7.2) and therefore  $v (= C_t/10) = 2.47\text{E}2$  m/s. The effective mass  $m^* = (W_0/L)/C_t^2 = (2.6\text{E}-9 \text{ J/m})/(2.47\text{E}3 \text{ m/s})^2 = 4.3\text{E}-16$  kg/m and therefore the (kinetic energy/b) is 0.051 J/m. This is less than  $\gamma$  (0.6 J/m<sup>2</sup>) and therefore the kinetic energy is insufficient to create the step.

The result is of interest for grain boundary hardening and is relevant to the Frank reflection mechanism for dislocation multiplication, Chap. 21.

- 7.7 Prove that the elastic displacements for a uniformly moving screw satisfy Eqs. 2.2 if one includes an inertial term

$$f_i = \rho_0 (\partial^2 u_i / \partial t^2)$$

## CHAPTER 8: THE INFLUENCE OF LATTICE PERIODICITY

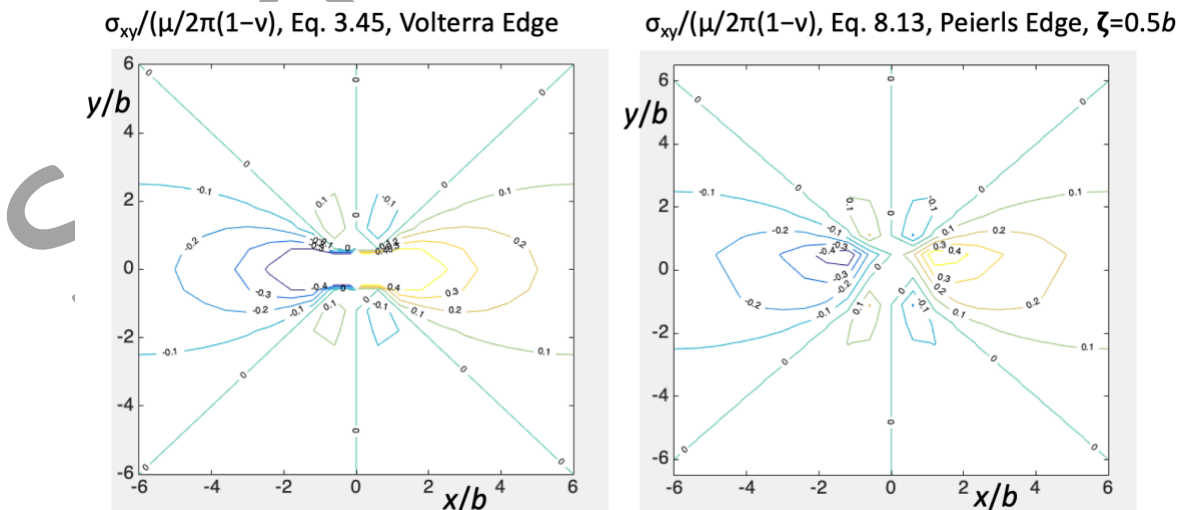
**Description:** These problems consider the effects of a Peierls (diffuse core) description of a dislocation on the stress field, cross slip, resistance to motion, and dissociation of dislocations. Estimates of kink widths, kink separation distances, and interaction energy between a kink and jog are also discussed.

- 8.1★ Graphically compare the results of Eqs. 3.45 and 8.13 for the stress  $\sigma_{xy}$  about an edge dislocation. For copper, at what distance from the core do the results differ by 20%? What is the value of the elastic strain at this position?

**MATLAB.** The stress field for a Peierls dislocation does not diverge at the actual origin as it does as is the case for the Volterra dislocation and thus the Peierls dislocation is more realistic in the core region. Specifically, the field above the glide plane is equivalent to that of a virtual Volterra dislocation with an origin a distance  $\zeta$  below the glide plane, and similarly the field below the glide plane is equivalent to that of a virtual Volterra dislocation with an origin above the glide plane.

The accompanying figure to Prob. 8.1 shows contour plots of normalized  $\sigma_{xy}$  for the Volterra (left) and Peierls (right) edge dislocations using Eqs. 3.45 and 8.13, respectively. For the Peierls case,  $\zeta = \pm 0.5 b$  where  $\zeta = +0.5$  for  $y \geq 0$  and  $\zeta = -0.5$  for  $y < 0$ . See the text just before Eq. 8.13.

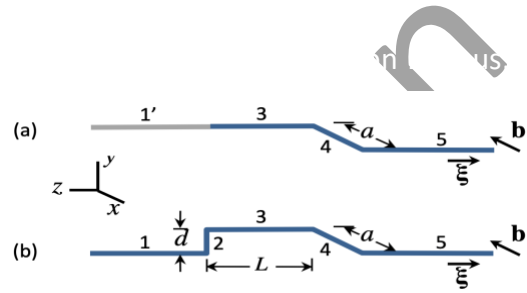
The results show that the 0 and  $\pm 0.1$  contours for both cases are similar but the  $\pm 0.2$  contours differ modestly and the difference increases for larger magnitude (e.g.,  $\pm 0.3$ ) contours closer to the center of the dislocation. For the Peierls case, the maximum shear stress of  $\sim 0.5$  occurs away from the center whereas for the Volterra case, the stress is singular at the origin. The two solutions differ by 20% approximately in the vicinity of the  $\pm 0.2$  contours which span up to  $5b$  from the center.



Problem 8.1.

- 8.2 Compare the tendency to cross slip for a Peierls dislocation vs. a Volterra dislocation.
- 8.3 Atomic binding is often described in terms of central forces that act between atom centers and resist changes in bond length, and directional forces that resist changes in bond angle. The former are predominant in close-packed metals. Discuss how each type of force affects the width  $\zeta$  of a Peierls dislocation and the width  $w$  of a kink. Classify fcc metals, bcc metals, ionic crystals, covalent crystals, and van der Waals crystals in order of increasing Peierls barrier.
- 8.4★ Discuss the qualitative differences in the magnitudes of the kink width and kink energy between kinks, based on the approximate energy relations in Figure 8.9 and the exact relations.  
The sinusoidal potential is "hard" compared to more realistic potentials. Thus, the sinusoidal potential almost certainly overestimates the Peierls barrier. Nevertheless, as discussed in the text, such a potential can be used as an empirical fit.
- 8.5 Calculate the equilibrium separation between the kinks in a kink pair, assuming a pure screw dislocation with an applied resolved shear stress  $\sigma = 10^{-5} \mu$ .
- 8.6 Consider three like-sign kinks in an edge dislocation, piled up against a pinning point that locks the first kink. The applied stress is  $\sigma = 10^{-4} \mu$ . What are the kink separations?

- 8.7☆ Estimate the width of kinks in screw dislocations in aluminum. Assume that  $\sigma_p = 10^{-5} \mu$ .  
MATLAB. The kink width  $w = a(W_0/2W_p)^{1/2}$  (Eq. 8.73), where: the kink height  $a$  (see Fig. 8.17) is approximated as  $b$  ( $= 2.86\text{E-}10$  m, based on  $a_{\text{Al}}/\text{sqrt}(2)$ , where the lattice parameter for Al is  $a_{\text{Al}} = 4.05\text{E-}10$  m); the dislocation line energy per unit length is  $W_0/L = (\mu b^2/4\pi)\ln(R/r_0) = 2.65\text{E}10$  J/m (Eq. 3.13), using  $R/r_0 = 200$ ; and the Peierls energy  $W_p/L = \sigma_p ab/\pi = 6.92\text{E-}15$  J/m (Eq. 8.44). The resulting kink width is  $w = 7.4\text{E-}8$  m, which is  $\approx 250 b$ . The large value of  $w/b$  is consistent with a small kink angle  $\psi$  (Fig. 8.17). The small  $\psi$  justifies the use of Eq. 8.73.
- 8.8☆ Based on the Peierls-Nabarro model and elastic isotropy, would the core of a  $\langle 110 \rangle$  screw dislocation dissociate on a  $(0\ 0\ 1)$  plane or on a  $(1\ \bar{1}\ 0)$  plane in a NaCl structure? Which slip system would have a smaller Peierls barrier? Which is observed experimentally (see Chap. 12)?  
See Fig. 12.14. The interplanar spacing is larger for the  $(1\ \bar{1}\ 0)$  plane so the Peierls model would predict a smaller barrier for that plane, in agreement with experiment.
- 8.9☆ Discuss whether the difference in energy between positive and negative kinks in mixed dislocations is important for phenomena other than those involving interaction with an external surface.  
The difference would favor a bias in the bow-out associated with groups of kinks. One type of kink would be favored if the kinks nucleated heterogeneously where a dislocation intersected a grain boundary, for example.
- 8.10☆ In view of the symmetry on an atomic scale, show that the Peierls barrier for  $(1\ 1\ 1)$  screw dislocations in  $\{1\ 1\ 0\}$  and  $\{1\ 1\ 2\}$  planes is asymmetric (Hirth and Lothe 1966).  
See the reference in the textbook for the solution.
- 8.11☆ Discuss the physical justification for defining Eq. 8.6 by its principal value.  
Without the use of the residue method, the integrals would be indeterminate, diverging as  $x \rightarrow 0$ .
- 8.12 Compute the elastic interaction energy between an oblique kink and a right-angle jog.



Problem 8.12.

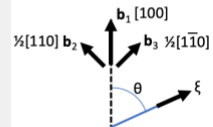
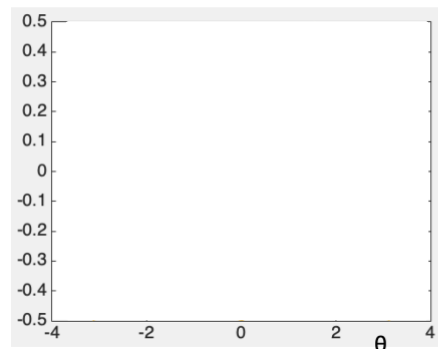
8.13 Would it be physically meaningful to invoke a Peierls model for dislocation climb?

### CHAPTER 9: SLIP SYSTEMS OF PERFECT DISLOCATIONS

**Description:** These problems consider the stability of dislocations to dissociation, the effect of  $c/a$  ratio on the Peierls stress in hcp crystals, calculation of the resolved shear stress on specific slip systems, independent slip systems, and compatibility across grain boundaries.

9.1 For what range of orientations should a dislocation with  $\mathbf{b} = [1\ 0\ 0]$  be stable in a fcc crystal? The analysis should include the variation of energy with screw-edge character.

$$\frac{F_g/L}{\mu b^2/2\pi R}$$

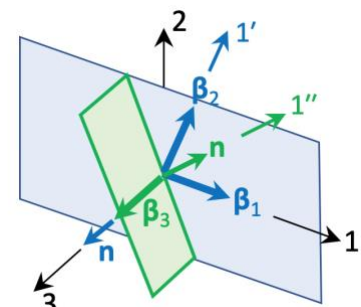


Problem 9.1.

- 9.2 For the hcp slip systems listed in Table 9.3, explicitly estimate the dependence of the Peierls stress on the  $c/a$  ratio. What is the effect of a superposed isostatic pressure on the Peierls stress?
- 9.3☆ Compute the resolved shear stresses on slip systems of the type  $\langle 1\ 1\ \bar{2}\ 0 \rangle \{1\ 0\ \bar{1}\ 0\}$  if a uniaxial compressive stress acts in the  $[1\ 1\ \bar{2}\ 3]$  direction in an hcp single crystal. Note: The corrections (in red text) to properly specify the slip direction with  $\langle \rangle$  and to ensure that  $l = -(h + k)$ . There are also errors in Table 9.3 that do not satisfy  $l = -(h + k)$ .  
For the solution to the problem, consider the example with slip direction  $\mathbf{b} = [1\ \bar{2}\ 1\ 0]$  and slip plane normal  $\mathbf{n} = [1\ 0\ \bar{1}\ 0]$ . Use Eq. 9.6 (or fig. 9.10 if a pole figure is available) to compute the resolved shear stress  $\sigma'_{12}$ . In this case, the dot product  $T_{11}$  between the slip direction and compression axis  $[1\ 1\ \bar{2}\ 3]$  is 0 and thus  $\sigma'_{12} = 0$ . This is just one example; other slip systems in the  $\langle 1\ 1\ \bar{2}\ 0 \rangle \{1\ 0\ \bar{1}\ 0\}$  family can produce  $\sigma'_{12} \neq 0$ .
- 9.4 Compute the resolved shear stresses on the  $[1\ \bar{1}\ 0]$   $(1\ 1\ 1)$  and  $[0\ 1\ 1]$   $(1\ \bar{1}\ 1)$  slip systems in a fcc crystal if a uniform torque is applied about the  $[1\ 1\ 2]$  axis.

9.5 How many independent slip systems exist in a simple cubic structure in which the allowed slip planes are the cube faces and the allowed slip directions are the cube edges?

9.6 Consider three slip systems with slip vectors  $\beta_1$ ,  $\beta_2$ , and  $\beta_3$ . Let  $\beta_3$  be normal to  $\beta_1$  and  $\beta_2$ , and let  $\beta_1$  and  $\beta_2$  have a common slip plane. Assume that the glide plane for  $\beta_3$  is any plane containing  $\beta_3$ . Are the three slip systems independent?



Problem 9.6.

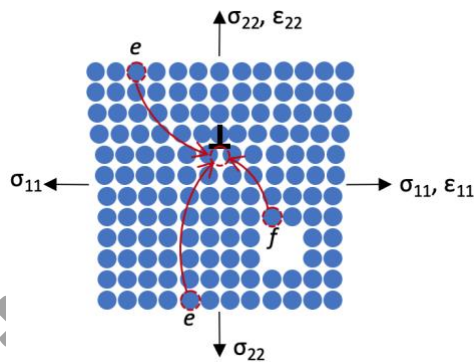
9.7 ☆ Consider the same case as in Prob. 9.6 except that  $\beta_3$  is not normal to  $\beta_1$  and  $\beta_2$ . Are the slip systems independent?

Yes. This is a more general case of Prob. 9.6.

9.8 ☆ In Prob. 9.6, is there a special choice of slip plane for  $\beta_3$  such that a purely longitudinal strain in the  $\beta_3$  direction would be impossible?

No. For any plane containing  $\beta_3$ , the slip system cannot produce the strain component  $\epsilon_{33}$ .

9.9 Discuss how climb processes modify the requirement for independent slip systems.



Problem 9.9.

- 9.10☆ For the bicrystal in [Figure 9.18](#), what orientations would require only one slip system in each crystal? Would elastic anisotropy change the result? Note the correction in the question statement (red text).

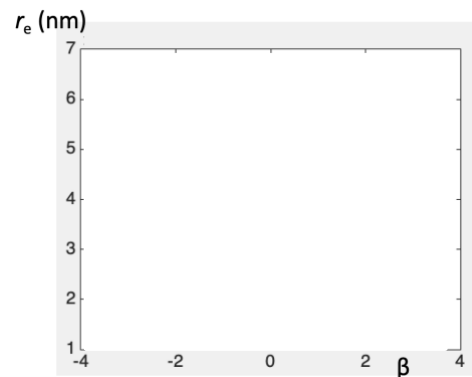
Consider a Cartesian coordinate system with  $x$  and  $z$  in the plane of the grain boundary and  $y$  normal to it, as shown in [Figure 9.18](#). Eq. 9.23 states that the strain components  $\epsilon_{xx}$ ,  $\epsilon_{zz}$ , and  $\epsilon_{xz}$  ( $= \epsilon_{zx}$ ) must be continuous across the grain boundary to avoid sliding or opening up/interpenetration of material at the boundary. This can be satisfied by one slip system in each grain if the components of Burgers vector  $b_x$ ,  $b_z$  and components of slip plane normal  $n_x$ ,  $n_z$  are equal for both slip systems. This would be satisfied, for example, if the grain boundary is a mirror plane. In general, the components  $b_y$  and  $n_y$  do not need to be equal for both slip systems.

The statement of compatibility above holds for the total strain, which can be partitioned into elastic and plastic contributions. If the grains are elastically anisotropic, it is possible that the components of elastic strain alone and the components of plastic strains alone do not satisfy Eq. 9.23 but the total strain components must. In such cases,  $b_x$ ,  $b_z$  and  $n_x$ ,  $n_z$  could be different. During plastic deformation, the plastic strains can become much larger than elastic strains in which case  $b_x$ ,  $b_z$  and  $n_x$ ,  $n_z$  must be the same in grains  $A$  and  $B$ .

## CHAPTER 10: PARTIAL DISLOCATIONS IN FCC METALS

**Description:** These problems consider a variety of analyses involving partial dislocations, including the equilibrium separation distance between partials, reactions involving stacking fault tetrahedra, partials bounding intrinsic and extrinsic faults, extended nodes, cross slip of extended dislocations, and other geometries.

- 10.1 Determine the variation with orientation of the equilibrium separation of partials bounding an intrinsic stacking fault in copper.



Problem 10.1.

- 10.2 Using the  $\gamma_i$  values from Appendix 2, find which fcc metals should have meaningful partial dislocation extensions; that is,  $r_e > 2b$ .

- 10.3 ☆ In terms of nearest neighbor bond energies  $\phi_1$ , evaluate the stacking fault energy associated with
- Climb of a Shockley partial
  - Glide of the stair rod  $\alpha\delta$
  - Glide of a Frank partial

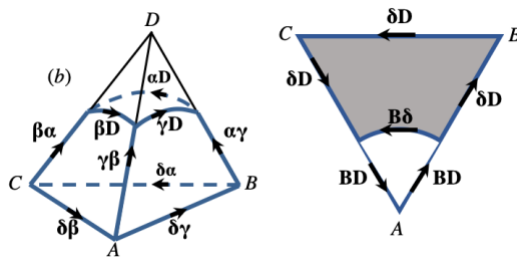
For all three cases, three near-neighbor bonds are severely distorted. The direct climb is most unlikely.

- 10.4 ☆ Draw the various stages of the advance of a  $\langle 1\ 1\ 0 \rangle$  jog line by absorption of a vacancy. The jog line is equivalent to a row of  $\frac{1}{3}$  vacancies. Absorption of a vacancy advances a length of 3 atom spacings by an atomic distance normal to the jog line and parallel to the glide plane, creating a kink on the jog line. Eventually, with more absorption, the jog line is displaced by one atomic distance.
- 10.5 ☆ Discuss the possible reactions that would produce a tetrahedron from a triangular interstitial disc. What configuration would form if the Frank partial bounding the disc dissociated directly to form a Shockley partial bounding an intrinsic fault?

Use Fig. 10.10 with  $D\delta$  as the Frank partial. There are three places on the loop where a tetrahedron could start to form. For example, a reaction is  $D\delta = D\gamma(c) + \gamma\delta$ , as in Fig. 10.26. The Frank partial could not glide but it could act as a source for a glissile dislocation by reacting to form a stair rod and a perfect dislocation: for example,  $D\delta = DB + B\gamma$ .

- 10.6 Label the dislocations in Figure 10.28 using the Thompson notation.

- 10.7 ☆ Show that simultaneous glide collapse from two corners of an intrinsically faulted tetrahedron results in a perfect  $\frac{1}{2}\langle 1\ 1\ 0 \rangle$  dislocation loop (Kuhlmann-Wilsdorf 1965).

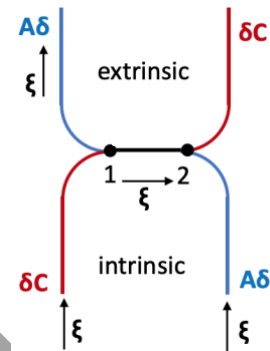


Problem 10.7.

The accompanying figure (left image) shows the collapse of a stacking fault tetrahedron at point  $D$ ; it is the reverse of the process shown in Fig. 10.26. When the segments  $\beta D$ ,  $\gamma D$ , and  $\alpha D$  reach the base of the tetrahedron, a stacking fault (gray region) is produced with dislocations of Burgers vector  $\delta D$  and counterclockwise sense  $\xi$  bounding the fault. The right image shows if a partial dislocation  $B\delta$  nucleates from point  $A$ , the fault is removed

(white region) and a perfect  $\frac{1}{2}\langle 1\ 1\ 0 \rangle$  dislocation loop results. The combined process involves the collapse from *D* and *A*.

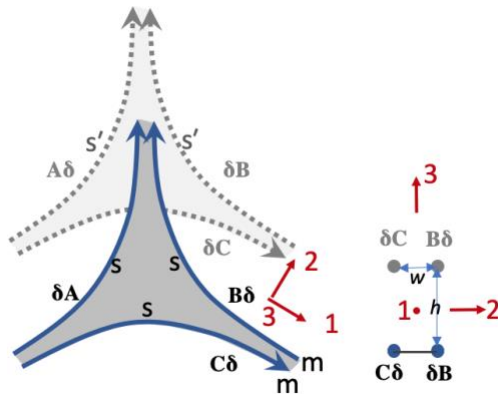
- 10.8 Consider the dissociation of dislocation **AC**(*d*) into an intrinsic stacking fault over some length, after which it dissociates into an extrinsic stacking fault on the same  $\{1\ 1\ 1\}$  plane. What partial crosses the dislocation where the change occurs?



Problem 10.8.

- 10.9☆ Consider an extended dislocation node that is parallel to a free surface. Determine whether the image forces increase or decrease the apparent value of  $\gamma_i$ .

The image forces are expected to constrict the node, which corresponds to an increase in the apparent stacking fault energy (see Sec. 10.4d). The direction of the image forces can be rationalized by constructing an extended node and its image as shown in the accompanying figure (the real node is in the foreground and the image is offset for visibility: it actually superposes on the real node when viewed normal to the surface). The signs of the image forces can be deduced more easily in the piecewise straight approximation of Fig. 10.33.



Problem 10.9.

There are two approaches to rationalize why the image exerts forces that cause the extended node to constrict (i.e., shrink the gray faulted region). In the first approach, the accompanying figure (left) shows that the partials **Bδ**, **Cδ**, and **δA** have pure screw character at the sites marked *s*. They repel one another; this must be so as to oppose the constricting force that arises from the stacking fault energy. Specifically, **Bδ** is repelled by **Cδ** and **δA**. At sites *s'*, the image dislocations are also pure screw but opposite in sign to their real counterparts. Thus, **Bδ** must be attracted by the images **δC** and **δA** and the node contracts. A similar effect occurs for dislocations **δA** and **Cδ**.

In the second approach, equilibrium is considered at one of the “arms” of the extended node, indicated by the sites marked *m*. The inset to the right a view along the arm, where the sense  $\xi$  for all dislocations (real and image) points along the 1-axis. Dislocation **δB** experiences a force in the 3-direction from the oppositely signed image

dislocation  $\delta\mathbf{B}$ ; this does not expand or contract the extended node. However, image dislocation  $\delta\mathbf{C}$  has an oppositely-signed screw component and like-signed edge component to  $\delta\mathbf{B}$  (See the Thompson tetrahedron, Fig. 10.10). Oppositely-signed screw components generate an attractive radial force and thus there is a force in the  $-z$  direction on  $\delta\mathbf{B}$ , constricting the node. The edge component also exerts a force in the  $-z$  direction on  $\delta\mathbf{B}$ , provided the extended node is sufficiently far from the surface for  $h > w$ . This geometric aspect is confirmed by consulting the plot of the stress field around an edge dislocation (Fig. 3.11) and also Prob. 3.20. Under such conditions, the stable equilibrium position for two like-signed edge dislocations occurs when they are vertically stacked above one another. The combined screw and edge contributions are such that the image  $\delta\mathbf{C}$  exerts a glide force in the  $-z$  direction on  $\delta\mathbf{B}$ , thus constricting the node. For similar reasons, the glide component of the image force on  $\mathbf{C}\delta$  is in the  $+z$  direction.

- 10.10☆ Consider the node between the dislocations  $\mathbf{AC}$ ,  $\mathbf{BA}$ , and  $\mathbf{CB}$  in the  $(d)$  plane. The dislocations are ribbons of intrinsic stacking fault and the order of the branches is such that the node would be contracted unless an extrinsic stacking fault forms at the node. Show how the node could become extended by the formation of an extrinsic fault. Fig. 19.28b shows a sequence leading to the formation of a hexagonal extrinsic stacking fault in the center.
- 10.11☆ Consider the intrinsically dissociated dislocation  $\mathbf{AC}(d)$ . Describe the possible superjogs that can dissociate into extrinsic faults on the  $(c)$  plane. In Fig.10.17, if one nucleates a loop  $\gamma\mathbf{C}$  on the jog fault, the end partial is converted from  $\gamma\mathbf{A}$  to  $\mathbf{B}\gamma$ . Similarly, the stair-rod converts to  $\gamma\delta/\mathbf{AB}$ .
- 10.12☆ Consider a dissociated screw with an intrinsic fault as it cross slips onto a conjugate plane without contracting. Describe the intermediate dissociated configuration. Would cross slip be easier if the screw dissociated extrinsically on the conjugate plane? Consider the dissociation of  $\mathbf{AB}$  into  $\delta\mathbf{B}$  on the left and  $\mathbf{A}\delta$  on the right, viewed from outside the tetrahedron (Figs. 10.9, 10.10) along the positive sense. The cross-slip dissociation of the leading partial is  $\mathbf{A}\delta \rightarrow \mathbf{A}\gamma + \gamma\delta$ , viewed along the positive sense. The Escaig mechanism, Fig. 27.18c, is most likely.
- 10.13 Could twinning occur by the formation of successive layers of extrinsic fault? If so, what shear would accompany twinning?
- 10.14 Consider an isolated Shockley partial in copper. Use Eq. 8.41 to compare the magnitude of force caused by the Peierls stress vs. that associated with the stacking fault.

10.15 Discuss the stability of the partial  $\mathbf{D}\gamma/\mathbf{A}\mathbf{C}$  that can form by the reaction of  $\mathbf{D}\mathbf{C}$  and  $\gamma\mathbf{A}$ .

### CHAPTER 11: PARTIAL DISLOCATIONS IN OTHER STRUCTURES

**Description:** These problems consider candidate twin planes in fcc and hcp structures, the formation of extended jogs, effects of dissociation on core structure, equilibrium spacing between partials, and considerations for ordered alloys.

11.1 Why is the basal plane in hcp metals not a twin plane, like the close-packed plane in fcc metals? What is the formal definition of twinning?

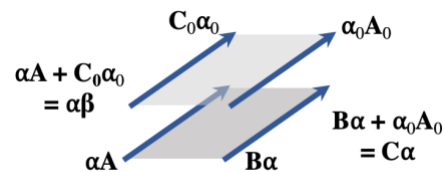
11.2 Show that  $(1\ 0\ \bar{1}\ 2)$  is a possible twin plane in hcp structures.

11.3☆ Consider the dislocation  $\mathbf{A}\mathbf{C}$  in the basal plane of an hcp metal. If the dislocation contains a jog that is an uneven number of plane spacings high, can the jog extend in a fashion similar to the jog in Figure 11.12? What partials result?

The jog plane is  $(1\ 0\ \bar{1}\ 0)$ . As in Fig. 9.5 (p. 239), this plane produces a zig-zag structure. The two vectors connecting the black atoms in Fig. 9.5 are not translation vectors but rather  $\epsilon\mathbf{C}$  type partials (see Table 11.1, p. 288). Therefore, dissociation is possible but the probability is likely to be small because the fault energy is likely to be large.

11.4☆ Show that dislocations  $\mathbf{A}\mathbf{C}$  and  $\mathbf{B}_0\mathbf{C}_0$ , lying on adjacent basal planes, can combine to form a configuration resembling that in Fig. 10.8b. What are the resultant partials and types of stacking faults? Note the correction in the question statement (red text).

An example is shown in the Figure. The fault is an extrinsic fault. Note the sense vectors are opposite to those in Fig. 11.2, which should point out of the page.



Problem 11.4.

11.5 Draw models for the core of a pure screw dislocation  $\mathbf{b} = \frac{1}{2}\langle 1\ 1\ 1 \rangle$  in a bcc structure, with the core dissociated on the  $(1\ \bar{1}\ 0)$  plane. Show that the core structure is different above and below the slip plane.

11.6 Devise a rule for the proper stacking sequence in the construction of the extrinsic fault, Eq. 11.8. For example, the inserted layer  $EF$  cannot be put between  $C$  and  $D$  as to produce the sequence  $ABCEFDE$ . Explain why.

11.7☆ Apply Eq. 10.14 to the bcc dissociations of Figure 11.14. Develop explicit expressions for the equilibrium partial spacing  $r_e$  and determine the proper dissociation to form the fault  $I_3$ .

A polynomial can be developed to balance the Peach-Koehler force  $F_{PK}/L$  on a dislocation arising from the stress field of all other dislocations with the force  $F_V/L = -\gamma$ , where  $\gamma$  is the energy/area of the fault between the two dislocations bounding the fault. The negative sign denotes that  $F_V/L$  acts to attract the bounding dislocations to one another.

11.8☆ Which jogs in Figure 11.30 can be formed directly by an intersection process?

Only the jog in Fig. *a* can be formed by intersection. The jog heights in Figs. *b* and *c* can only be formed by intersections with  $A_e$  type partials, which perform are not translation vectors.

11.9 Could a junction of four antiphase boundaries exist in  $\beta$ -brass? Could it dissociate; that is, would any two of the four domains be in phase? Are such junctions expected after deformation? After annealing, which junction allows atom regrouping?

11.10 Discuss the likelihood of dissociations to form  $\frac{1}{6}\langle 1\ 1\ 1 \rangle$  partials on  $\{1\ 1\ 2\}$  in ordered  $\beta$ -brass.

11.11☆ Figure 11.38a shows a superdislocation containing dislocations with collinear Burgers vectors. It contains a jog and a stepped antiphase boundary (APB). The jogs in each

component dislocation lie in the same (yz) glide plane, so if the dislocation moves in the y direction, the trailing dislocation annihilates the antiphase boundary created by the leading dislocation. The superdislocation in Figure 11.38b is composed of dislocations with jogs that are misaligned in the x direction. Show that motion of this superdislocation creates a rectangular tube of antiphase boundary (Vidoz and Brown 1972).

The cited reference (see the text. p. 686) details the solution.

## CHAPTER 12: DISLOCATIONS IN IONIC CRYSTALS

**Description:** These problems consider for ionic crystals the effective charge along edge and screw dislocations as well as at jogs and kinks, and implications for mobility and cross slip.

**Unless otherwise stated, the problems refer to the NaCl structure.**

12.1 Suppose that a square prismatic loop with Burgers vector  $\mathbf{b} = [\bar{1} 0 1]$  and edges along  $[0 1 0]$  and  $[1 0 1]$  forms by vacancy condensation. What is the magnitude of the effective charge of the corners?

12.2★ Suppose that the jog in the screw in Figure 12.19 has an effective charge  $q_c - e$ , but this changes to  $q_c + e$  after moving one step forward. How is the charge balanced during such motion?

The crystal is divalent, e.g., MgO. The jog carries a unit charge. If it is negative, it could convert to a positive charge either by the addition of a doubly-charged Mg cation (cation vacancy emission) or by the emission of a doubly-charged Cl anion (anion vacancy absorption).

12.3 If screws with Burgers vector  $\mathbf{b} = [1 0 0]$  existed, would kinks and jogs in such screws be charged?

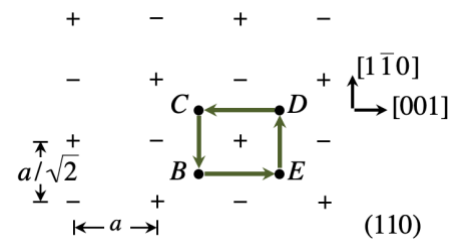
12.4★ Consider an edge dislocation with  $\mathbf{b} = [1 0 1]$  moving through a monatomic surface ledge lying along  $[0 0 1]$  on  $(0 1 0)$ . Determine the charge of the kink in the ledge and derive the charge balance for the process.

Sites along the ledge have charges  $\pm e/2$ . The dislocation cuts the ledge and leaves a surface kink in it. The charge on the kink is  $\pm e/2$  and it oscillates in sign if it propagates along the ledge.

12.5 Should the accumulation of jogs of one sign of charge affect the tendency of a screw dislocation gliding on  $(1 1 0)$  to cross slip onto  $(0 0 1)$ ? Why?

- 12.6 A NaCl single crystal is bounded by  $\{1\ 0\ 0\}$  faces and compressed along  $[0\ 0\ 1]$ . Suppose that slip occurs by the motion of only pure edge and pure screw dislocations.
- What predominant type of intersection jog should be formed?
  - Which set of dislocations is more mobile: screws or edges?
  - Which set of dislocations, screws or edges, can produce transient electrical currents during glide?
- 12.7☆ Consider a CsCl or  $\beta$ -brass type of ionic crystal that slips on the systems  $\langle 1\ 0\ 0 \rangle \{1\ 1\ 0\}$ . Determine whether or not the following defects are charged: screw jogs, screw kinks, edge jogs, edge kinks.

Consider the case of monovalent CsCl analogous to NaCl in Fig. 12.1, where  $\text{Na}^+$  is replaced by  $\text{Cs}^+$ . The structure is an interpenetrating simple cubic structure instead of interpenetrating fcc. The accompanying figure (reproduced from Fig. 12.14) shows that if a screw dislocation with  $\mathbf{b}$  and  $\xi$  out of the paper were to glide on path  $BE - ED - DE - CB$ , a closed path would result and the column of material inside the loop would shift out of the paper, producing charge transport. The  $\text{Cs}^+$  atom at the top of the column signifies a transport of charge of  $+e$  in the direction out of the plane of the paper. Motion of the screw along each leg of the circuit would contribute to the charge transport:  $q_g$  along the primary glide planes  $ED$  and  $CB$  and  $q_c$  along the cross slip planes  $BE$  and  $CD$  (see Sec. 12.4a). The simplest approximation is that  $q_c = q_g = +e/4$ . If instead the path enclosed a  $\text{Cl}^-$  atom, then  $q_c = q_g = -e/4$ . More likely, because of the symmetry,  $q_c \neq q_g$  but still  $q_c + q_g = e/2$ .



Consider a pure screw dislocation that is gliding along the path  $BE$ .

- The glide of a kink  $BE$  on the screw gliding on the primary slip plane, transports charge  $q_c$  in the  $[1\ 1\ 0]$  direction, eventually emerging at the surface and propagating a surface step (see Sec. 12.4b)
- The glide of a kink on the screw gliding on the cross-slip plane, transports charge  $q_g$  in the  $[0\ 0\ 1]$  direction.
- The kink on the cross-slip plane is a jog relative to motion on the primary glide plane. If the screw moves in the  $[1\ \bar{1}\ 0]$  plane, the jog will be sessile and can only move by

absorbing/emitting a vacancy or interstitial. If it moves, it changes sign. Therefore, the screw jog has charge  $\pm e/2$ .

Motion of a kink on an edge dislocation does not change or transport any charge so  $q = 0$  (slip occurs in the plane of the surface and thus there is no charge transport to the surface. See Fig. 12.13).

- Formation of a jog on an edge:  $\pm e/2$  (this requires diffusion of atoms or vacancies to the dislocation. Transport of a  $\text{Cs}^+$  ion to the dislocation core or a vacancy to replace a  $\text{Cs}^-$  ion at the core transports a charge of  $+e$  to the dislocation. See Sec. 12.3d. In the case of a jog pair, the charge of  $e$  is proportioned between the two jogs.

12.8 Should superjogs tend to form in MgO? In PbS? Discuss the role of polarizability in superjog formation.

12.9☆ What is the charge on the (0 0 1) surface at the point of emergence of a screw dislocation along [1 0 1]? The surface ledge lies along [0 1 0] and is shown in Fig. 12.19.

The exact geometry differs from that in Fig. 12.19 in that Burgers vector and dislocation line are not perpendicular to the surface. Along the ledge, the ions alternate in sign. If the ledge moved all the way across the crystal, two new corners, each with charge  $\pm e/8$  would be created. Therefore, the point of emergence has charge  $\pm e/8$ .

Another way to rationalize the answer is to modify the figure for Prob. 12.7 to represent a (0 0 1) surface. In that case the  $\text{Na}^+$  and  $\text{Cl}^-$  ions would form a square instead of rectangular pattern, and motion of a screw dislocation with Burgers vector along [1 0 1] around the path  $BEDCB$  would shift a  $\text{Na}^+$  ion out of the surface, equivalent to charge transport  $e$  along the dislocation. Thus, slip along the portion  $BE$  only would be  $1/4$  of the total circuit and a charge transport of  $e/4$  would result. The slip along  $BE$  could be accomplished by inserting two oppositely signed screw dislocations at the midpoint of  $BE$  and expanding the dipole so that one dislocation resides at  $B$  and the other at  $E$ . A charge transport of  $e/4$  would result, equivalent to a charge of  $e/8$  at the point of emergence of each screw dislocation. If the dipole were expanded further, e.g., by moving the dislocation at  $E$  one unit distance to the right, a negative ion would be displaced out of the surface, equivalent to a charge transport of  $-e/4$  along the moving dislocation. The charge at the point of emergence of the displaced dislocation would be  $-e/8$  ( $= e/8 - e/4$ ). Thus, the charge at the point of emergence would fluctuate from  $+e/8$  to  $-e/8$  during glide along a cube direction.

## CHAPTER 13: DISLOCATIONS IN ANISOTROPIC ELASTIC MEDIA

**Description:** These problems involve the computational of elastic constants along directions relevant to slip systems and examples of anisotropic elastic effects on the interaction between partials.

- 13.1★ Compute the components  $s'_{ij}$  of the compliance matrix for a cubic crystal, referred to the coordinates of Figure 13.2. Verify that  $\{s'\}$  is the inverse of  $\{c'\}$  for this case.

The 9x9 compliance matrix  $\{s'\}_{9 \times 9}$  with components referred to the coordinates of Figure 13.2 satisfies the same form as Eq. 13.35 so that  $\{s'\}_{9 \times 9} = \{Q\}_{9 \times 9}^T \{s\}_{9 \times 9} \{Q\}_{9 \times 9}$ , where the structures of  $\{s\}_{9 \times 9}$  and  $\{c\}_{9 \times 9}$  referred to the cubic crystal basis are given by Eq. 13.38 and the values of  $\{Q\}$  for the transformation from the cubic crystal basis to that in Figure 13.2 are provided by Eq. 13.37. This provides the necessary information to determine all of the components of  $\{s'\}_{9 \times 9}$  in terms of the components of  $\{s\}_{9 \times 9}$ .

To verify that  $\{s'\}_{9 \times 9}$  is the inverse of  $\{c'\}_{9 \times 9}$ , the above relations can be used to state  $\{s'\}_{9 \times 9} \{c'\}_{9 \times 9} = \{Q\}_{9 \times 9}^T \{s\}_{9 \times 9} \{Q\}_{9 \times 9} \{Q\}_{9 \times 9}^T \{c\}_{9 \times 9} \{Q\}_{9 \times 9}$ . One can show that  $\{Q\}_{9 \times 9} \{Q\}_{9 \times 9}^T = \{I\}_{9 \times 9}$  and thus the previous relation can be simplified to  $\{s'\}_{9 \times 9} \{c'\}_{9 \times 9} = \{Q\}_{9 \times 9}^T \{s\}_{9 \times 9} \{c\}_{9 \times 9} \{Q\}_{9 \times 9}$ . Finally,  $\{s\}_{9 \times 9} \{c\}_{9 \times 9} = \{I\}_{9 \times 9}$  and therefore the previous relation can be simplified to  $\{s'\}_{9 \times 9} \{c'\}_{9 \times 9} = \{Q\}_{9 \times 9}^T \{Q\}_{9 \times 9} = \{I\}_{9 \times 9}$ .  $\{s'\}_{9 \times 9}$  is therefore the inverse of  $\{c'\}_{9 \times 9}$ .

- 13.2★ Find the elastic-constant matrix appropriate to determine the energy of a  $\langle 11\bar{2}3 \rangle \{11\bar{2}2\}$  screw dislocation in an hcp crystal. What class of solution for  $p_n$  applies in this case?

See Teutonico LJ (1970) *Mater. Sci. Eng.* 6: 2747. The elastic constants are such that there is no simple solution in this case.

- 13.3★ Produce a polar plot of  $\sigma_{xx}$  and  $\sigma_{xy}$  for an edge dislocation with  $\mathbf{b} = \frac{1}{2}[101]$  and  $\boldsymbol{\xi} = [010]$  in NaCl. Compare the result with the isotropic results of Figure 3.12.

As in Exercise 13.9 (p. 361),  $\sigma_e = K_e b_e / 2\pi r$ . The elastic constants are in Eq. 13.42 and the stresses are given in Eq. 13.118 and 13.107. Polar plots with the x-axis  $\parallel \mathbf{b}$  can be made.

- 13.4 The following hcp elastic constants (Huntington 1958) are given in units of 10 GPa.

Metal	$c_{11}$	$c_{33}$	$c_{12}$	$c_{13}$	$c_{44}$	$K_{e(x)}$	$K_s$
Cd	12.10	5.13	4.81	4.42	1.85	3.43	2.60
Co	30.70	35.85	16.50	10.3	7.53	12.5	7.31
Mg	5.97	6.17	2.62	2.17	1.64	2.47	1.66
Zn	16.10	6.10	3.42	5.01	3.83	5.50	4.93

Compute the energy coefficients  $K_s$  and  $K_e$  for  $\langle 11\bar{2}0 \rangle (0001)$  dislocations in these metals.

- 13.5 a. Show that the separation widths between the partials of a 60° mixed dislocation in fcc crystals is  $r = K_e b^2 / 12\pi\gamma$ .

- b. Use this result to verify the results of Table 13.1 for the 60° dislocation.
- c. Compare the relative widths given in Table 13.1 to those given by Eq. 10.15. Do this for Al, Cu, Au, and Pb using the Voigt averages for  $\mu$  and  $\nu$ .
- d. Compare the above results with those obtained using the Reuss averages for  $\mu$  and  $\nu$ .
- e. Compare the above results with those obtained using the crude approximation  $\mu = c_{44}$  and  $\nu = 1/3$ .
- 13.6 Derive the formula for the equilibrium width of a  $\frac{1}{2}\langle 1\ 1\ 1 \rangle$  screw dislocation that dissociates into partials  $\frac{1}{3}\langle 1\ 1\ 1 \rangle$  and  $\frac{1}{6}\langle 1\ 1\ 1 \rangle$  bounding an intrinsic stacking fault in a bcc crystal.
- 13.7★ Show that the solution for  $p_n$  does *not* reduce to a third order equation in  $p^2$  if the dislocation lies along the threefold axis of a trigonal crystal. Why not?  
For trigonal crystals,  $c_{14} \neq 0$ . Thus, the reduction to the simple form of Eq. 13.97 is not possible.
- 13.8★ A screw dislocation in a cubic crystal lies along a  $\langle 1\ 1\ 0 \rangle$  direction parallel to a free surface. Discuss whether a simple image construction yields the correct force acting on the screw. Does the same reasoning apply for a  $\langle 1\ 1\ 1 \rangle$  screw dislocation?

The relevant stresses are those of Eqs. 3.3 and 13.129. In both cases,  $x$  is zero at the surface and the stresses are odd in  $y$ . Thus, the mirror image construction satisfies the free surface boundary condition. For a  $\langle 111 \rangle$  screw,  $\sigma_{rz}$  given in Eq. 13.158 does not vanish when the image stress is added and the simple image construction does not give the correct answer.

- 13.9☆ A  $\frac{1}{2}[111]$  partial dislocation lies along  $[1\bar{1}0]$  in a Cu crystal. Use a force balance to assess the likelihood of dissociation into the two partials  $\frac{1}{6}[112]$  and  $\frac{1}{6}[110]$ .

The mixed  $\frac{1}{2}[111]$  partial splits into a  $\frac{1}{6}[110]$  screw partial and a  $\frac{1}{6}[112]$  edge partial. Thus, as in Sec. 13.6, the stress fields are such that the two partials do not interact, at least based on the linear-elastic fields. Probably splitting would not occur, because the single core likely has a lower core energy than two cores. However, if the two partials were separated, they would not interact and would remain separated.

## CHAPTER 14: EQUILIBRIUM DEFECT CONCENTRATIONS

**Description:** These problems compute the entropy, effective mass, widths, concentrations, and interaction energies of kinks and the concentrations of vacancies and different solutes in the vicinity of dislocations, including the effects of elastic modulus mismatch between solutes and solvents.

- 14.1☆ a. For  $\omega = 10^{11}$  and  $10^{12} \text{ s}^{-1}$ , compute the  $T$  at which the entropy of the vibrational mode approaches the high  $T$  limit.

**MATLAB.** The expression for  $kT \gg \hbar\omega$  that follows Eq. 14.2 is rearranged to provide an equation for  $T$  through expansion of the exponential factor in high  $T$  limit:  $[1 - \exp(-\hbar\omega/kT)] \approx (\hbar\omega/kT) - (\hbar\omega/kT)^2$ . Setting this equal to 0.95  $(\hbar\omega/kT)$  provides an estimate,  $T = 20\hbar\omega/k = 1.5E1$  and  $1.5E2$  for  $\omega = 10^{11}$  and  $10^{12} \text{ s}^{-1}$ , respectively.

- b. If  $\omega_p = 10^{12} \text{ s}^{-1}$  and  $\omega_k = 10^{11} \text{ s}^{-1}$ , compute the kink entropy  $S_k$ . Compare the entropy contribution to  $F_k$  and the energy contribution at room  $T$  if  $2W_k = 0.3 \text{ eV}$ . At what  $T$  are the two contributions equal?

$S_k = 8.2E-23 \text{ J/K}$ , based on Eq. 14.4 with  $T_{\text{room}} = 293 \text{ K}$  and the prescribed values. The entropy contribution to  $F_k$  is  $TS_k$ , which equals  $2.4E-20 \text{ J} = 0.15 \text{ eV}$ . Thus,  $TS_k$  is approximately  $\frac{1}{2}$  of  $2W_k$  at room  $T$ . The two contributions are comparable at about  $T = 600 \text{ K}$ .

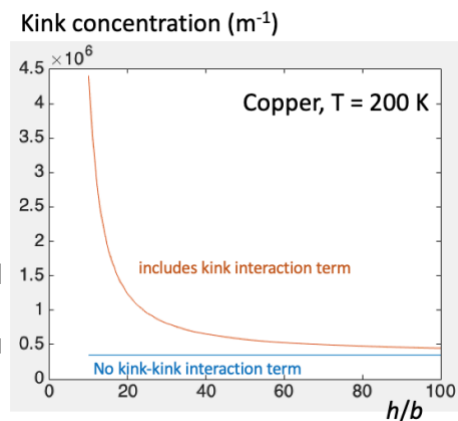
- c. Compare the result of Eq. 14.6 to that of (b) at room  $T$ , assuming an effective mass  $m^* = W_k/C_t^2$  of the kink and a typical value  $C_t \sim 10^5 \text{ cm/s}$ .

$S_k = 3.1E-23 \text{ J/K}$  based on Eq. 14.6 with  $a = 1E-8 \text{ m}$ ,  $h = 6.63E-34 \text{ kg m}^2/\text{s}$ ,  $T = 293 \text{ K}$ ,  $C_t = 1E5 \text{ m/s}$ , and  $W_k = 0.15 \text{ eV}$ . The resulting effective mass of the kink is  $m^* = 0.15 \text{ eV}/10^6 \text{ m}^2/\text{s}^2 = 2.4E-26 \text{ kg}$ .

- 14.2 Use Eqs. 8.40 and 8.80 to compute the approximate kink widths in copper, silver, and gold. Show the range of orientations for which a discrete kink model should apply for these metals, in terms of a polar plot of orientations in the slip plane.

14.3 Compute the concentrations of thermal kinks and thermal jogs in an otherwise straight dislocation line, for copper at 100, 300, and 900 K.

14.4☆ a. Include the kink-kink interaction energy in the free energy of formation of a kink pair, using the results of Chapter 8. Plot the equilibrium concentration of kink pairs as a function of separation distance  $h$ , for copper at 200 K. Over what distance does the interaction energy appreciably affect the kink pair concentration?



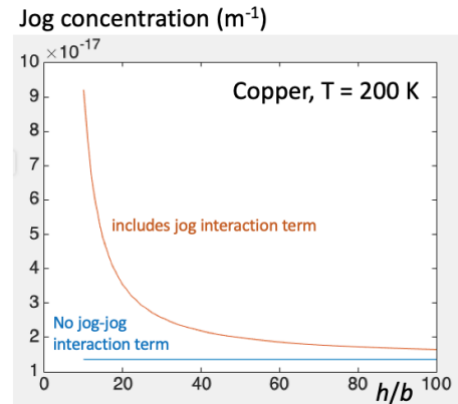
Problem 14.4a.

the plot shows the kink concentration without the interaction energy (blue) and with the interaction energy (red). The negative interaction energy increases the concentration as the kink separation distance,  $h$ , diminishes. The concentration is affected appreciably over the range shown here.

**MATLAB.** For copper,  $\nu = 0.327$ ,  $\mu = 5.46E10$  Pa, and  $b = 2.54E-10$  m for a  $\frac{1}{2}\langle 110 \rangle$  dislocation. The approximation  $a = b$  is used to estimate the interaction energy  $W_{int}$  (Eq. 8.51) and energy of formation  $2W_f$  (Eq. 8.50). The former is for a kink pair and thus it is negative. As noted in the discussion of Eq. 8.50, the small length of kinks introduces significant uncertainty in the estimate of  $2W_f$ . In the logarithmic factor,  $a/\rho = 6$  is used for the ratio of the kink height to cutoff, to ensure  $2W_f > 0$ . In the accompanying figure for Prob. 14.4a,

- b. Repeat the steps in (a) for jog pairs.

**MATLAB.** For the jog pair, the relevant relations are Eqs. 8.95 and 8.97. The accompanying figure shows a similar trend to that for kinks except that the concentrations are orders of magnitude smaller. The results are very sensitive to the choice of cutoff  $\rho$ . For example, changing  $a/\rho$  from 6 to 5 to 4 changes the concentration from  $1\text{E-}17$  to  $1\text{E-}11$  to  $1\text{E-}3\text{ m}^{-1}$ .



Problem 14.4b.

- 14.5 ☆ Consider two solute atoms that are near the

center of a large spherical crystal and

separated by distance  $h$ . Let  $v_s > v_a$ . Use the

results of Sec. 2.7 to show that there is *no* isostatic interaction between the two atoms in the absence of image stresses. Compute the isostatic interaction when image terms are present.

For an elastically deforming body, Eq 2.91 expresses the components of stress in terms of the radial displacement  $u_r$  and  $\partial u_r / \partial r$ , where  $u_r$  for a source of expansion in an infinite body is given by the first term in Eq. 2.90. Combining these, one finds that  $p = -(\sigma_{xx} + \sigma_{yy} + \sigma_{zz})/3 = 0$ . Therefore, if a solute atom is approximated as a point source of expansion in an infinite body, then the stress field generated by the solute atom involves shear components of stress but the internal pressure  $p$  is zero. If insertion of the second atom is modeled by a second point source of dilatation of magnitude  $\delta v$ , there is no  $p \delta v$  interaction between the two atoms. With an external surface at  $R$ ,  $p = -\alpha$ . The image term  $u_r = \alpha r$  and from Eq. 2.91 the pressure is  $p = -(3\lambda + 2\mu)\alpha$  and therefore a finite solute-solute interaction energy occurs. However,  $p$  and therefore the interaction energy is position independent, so there is no interaction force between the solute atoms. Eqs. 2.90 and 2.91 are written for a point source of expansion and thus the conclusions are valid in the limit where the separation distance between the atoms is much greater than the radius of the atoms.

- 14.6 ☆ Assume the isotropic continuum model result,  $V_v = v_v + v_c$ , for the external volume contraction associated with a **given** vacancy. Identify which volume terms would be measured in the following experiments and whether these terms would all be in agreement. Note the modification to the question statement (**red** text).

- a. Dilatometric determination of the lattice contraction accompanying the annealing out of vacancies at room  $T$  under zero external stress (Fraikor and Hirth 1967).

This measures the external volume change  $V_v$ .

- b. Pressure dependence of the quenched-in resistivity following quenching from elevated  $T$  under various pressures (Huebener and Homan 1963).

This is sensitive to only  $v_v$ .

- c. High- $T$  dilatometric measurements, subtracting out the effect of thermal expansion of the bulk lattice (Simmons and Balluffi 1962).

This measures the external volume change  $V_v$ .

Thus, the three measurements do not all measure the same quantity.

- 14.7☆ Consider a cylindrical crystal under uniform simple tension  $\sigma_{xx}$  parallel to the cylinder axis. Assume *local* vacancy equilibrium at the crystal surfaces. Compute the local equilibrium concentration at the surfaces where  $\sigma_{xx}$  is applied and at the lateral free surfaces where  $\sigma_{xx}$  is not applied.

At the lateral free surfaces where  $\sigma_{xx} = 0$ , there is no external work term when a solute atom moves to a surface kink and thereby creates a vacancy. At this surface  $c_v = c_v^0$ . At the surface where  $\sigma_{xx}$  is applied, the addition of an atom at the surface kink entails external work  $\sigma_{xx} A_x a$ , where  $A_x$  is the surface area of the atom and  $a$  is the displacement normal to the surface. Then, from Eq. 14.38,  $c = c_v^0 \exp(\sigma_{xx} A_x a/kT)$ . The vacancy concentration is increased if  $\sigma_{xx} > 0$  (tension) and decreased if  $\sigma_{xx} < 0$  (compression).

- 14.8 For the case of gold, compare the vacancy concentrations as a function of distance from a pure edge dislocation, as given by Eq. 14.39 vs. Eq. 14.45.

- 14.9 Compare the magnitudes of the energy terms in Eqs. 14.48 and 14.71 for Al dissolved in Cu, and also for Zn in Cu, Ag in Au, and Cu in Ni.

- 14.10☆ Determine from Eq. 14.77 the integral concentration of free lengths between  $l'$  and some value  $l''$  representing the average length of dislocation segments in a crystal. Compute the concentration of all lengths between  $l' = 10^{-6}$  cm and  $l'' = 10^{-3}$  cm at 100, 300, and 700 K. Assume bcc iron with one carbon atom per  $10^4$  possible bulk interstitial sites and the reasonable value  $F_B \sim 1.0$  eV. (Note the corrections shown in red text. The binding energy should be 1.0 eV, as discussed in a footnote in Sec. 18.5.)

**MATLAB.** Eq. 14.77 gives the number of clean segments of length  $l$  per unit length of dislocation, where  $a = b = 2.866 \times 10^{-10}$  m is used for BCC iron,  $\bar{G} \approx 0.8$  eV, and  $G_B = 1.0$  eV (see the discussion in Sec. 18.5 related to Wreidt, HA, Darken, LS (1965), *Trans. Metall. Soc. AIME* 233:122). The integral  $C = \int_{l'}^{l''} c_l dl$  from  $l'$  to  $l''$  gives  $C = [\exp(-ql') - \exp(-ql'')]/qb$ , where  $q = (G_B + \bar{G})/kTa$  with  $a = 1E4 b$ . The result is  $C = 2.3E-3$ ,  $1.1E-2$ , and  $3E-2$  for the cases  $T = 100, 300$ , and  $700$  K.

- 14.11 Determine the divalent impurity concentration that would give  $T_0 = 300$  °C in NaCl. Take  $v_a = 4.4 \times 10^{-23}$  cm<sup>3</sup> and  $W_v = 1.01$  eV (Etzel and Maurer 1950) and assume  $\Delta = 0.20$  eV.

- 14.12☆ Eq. 14.89 applies to the Debye-Hückel radius in the intrinsic range. Consider an extrinsic range with a divalent impurity concentration  $c^{++}$  and suppose all cation vacancies are quenched out. Estimate the Debye-Hückel radius if both divalent impurities and anion vacancies can rearrange themselves to provide an atmosphere.

**MATLAB.** Eq. 14.89 can be used to estimate  $\lambda$  in the absence of impurities, when cation vacancies are dominant. There,  $n$  is the concentration of ions, equal to  $1/\Omega$ , where  $\Omega$  is the volume per ion. Typical values for alkali halides such as NaCl are  $\Omega = 8.21E-30$  m<sup>3</sup> and  $\epsilon = 8$ . The fraction of vacancy sites,  $\alpha$ , is given by Eq. 14.85 with only  $F_c$  in the exponent, where  $F_c = 9.648E4$  J/mol is representative for alkali halides such as NaCl. At  $T = 400$  K,  $\alpha = 3.98E12$  and  $\lambda = 0.209$  nm. This provides very efficient screening. At  $T = 700$  K,  $\lambda = 180$  nm. The screening is less efficient because of the greater vacancy concentration and entropic spreading.

If the anion vacancy concentration is fixed by the divalent impurity fraction  $X = c^{++}/n$ , (see Eq. 14.104), then  $\alpha$  in Eq. 14.89 is replaced by  $X$ . As an example, if  $X = 0.001$ , then  $\lambda = 0.139$  nm and the screening is considerably greater. The intrinsic screening lengths increase with increasing temperature while the extrinsic lengths decrease weakly, in proportion to  $T$ .

- 14.13 Substitute a host atom with an incompressible atom having a volume  $\delta v$  larger than that of the host atom.
- Calculate the external expansion  $\delta V$ .
  - If an external pressure  $P$  is present, show that an extra amount of work  $P \delta V$  is required to insert the atom. *Hint:* If the crystal is compressed initially, a volume  $\delta v + Pv_a/B$  must be opened up to accommodate the inserted atom.
- 14.14☆ Consider the situation in Prob. 14.13 but assume a compressible substitutional atom with bulk modulus  $K' \neq K$ . Show that if an external pressure  $P$  acts, then the extra amount of work to insert the atom is again  $P \delta V$ .  
Eq. 14.46 is used with  $K' \neq 0$  to provide a first-order estimate of  $\delta V$ . More formally, the higher order work term would include  $\Delta v_a/v_a = P/K_a$  and  $\Delta v_s/v_s = P/K_s$  so that the higher order term is  $P(\Delta v_a - \Delta v_s)$ .

## CHAPTER 15: DIFFUSIVE GLIDE AND CLIMB PROCESSES

**Description:** These problems explore length scales for diffusion of vacancies, velocities of kinks and dislocations, the effect of stress on kink activation energy and vacancy concentration, and the collapse or expansion of vacancy loops.

- 15.1 Verify by direct substitution that the solution for concentration,

$$c = (4\pi Dt)^{-1/2} \exp(-x^2/4Dt)$$

satisfies the 1D diffusion equation  $\partial c/\partial t = D \partial^2 c/\partial x^2$  for all particles concentrated at  $x = 0$  at  $t = 0$ .

- 15.2 Discuss the time dependence of the solution in Prob. 15.1. Show that  $\langle x^2 \rangle = 2Dt$ .

- 15.3 Assume for a metal that  $D_v \cong b^2 v \exp(-W_v'/kT)$  (see Eq. 15.7),  $v = 10^{13} \text{ s}^{-1}$ ,  $b = 2 \times 10^{-8} \text{ cm}$ ,  $W_v' = 0.2 \mu b^3$ , and the melting point  $T_m = (2 \times 10^{-2}) \mu b^3/k$ . How far will a vacancy diffuse in 1 s at  $T$  just below the melting point?
- 15.4☆ Suppose that  $D_k$  is given by Eq. 15.11. How fast will the kink move relative to  $C_t$  at room  $T$  when acted upon by a force  $F \cong 10^{-4} \mu b^2$ , corresponding to a stress  $\sigma \sim 10^{-4} \mu$ ? Use the Einstein mobility relation and assume  $\mu b^3 = 5 \text{ eV}$ .  
**MATLAB.** Eq. 15.9a is used to estimate  $v_k$  and  $C_t \approx v_D b$ , so that  $v_k/C_t = \sigma b^2 h/kT$ . The result,  $v_k/C_t \approx 0.02$ , is obtained by taking  $\sigma = 1\text{E-}4 \mu$ , the kink height  $h = b$ ,  $T_{\text{room}} = 293 \text{ K}$ , and  $\mu b^3 = 5 \text{ eV}$ .
- 15.5 Find the velocity of a screw dislocation under the conditions of Prob. 15.4, with one kink per 30 kink sites in the dislocation. Assume  $a = h = b = 2 \times 10^{-8} \text{ cm}$ .
- 15.6☆ Consider a straight dislocation segment of length  $L$  lying in a Peierls valley. Suppose it can move to a kink pair configuration with kink separation  $\sim L$ . How large a resolved shear stress is required to change the energy of the kinked configuration by  $kT$  relative to the unkinked configuration? How large is this stress for  $L = 10^3 b$ ? For  $L = 10^2 b$ ? Assume  $kT \sim \mu b^3/400 \sim 0.012 \text{ eV}$  and  $h = b$ .  
**MATLAB.** Eq. 8.49 indicates that the change in energy to form a kink pair on a screw dislocation is  $W = 2W_f + W_{\text{int}}$ , where  $W_f$  is given by Eq. 8.50 and  $W_{\text{int}}$  by Eq. 8.51. If a shear stress  $\sigma$  acting on the slip plane in the direction of slip is present, then the energy change is  $W - \sigma b h L$  and this is equated to  $kT$ . The required shear stress is  $\sigma = (W - kT)/b h L$ . This can be normalized so that  $(\sigma/\mu)(L/b) = [1/2\pi(1-\nu)][\ln(a/\rho) - (1-\nu)] - [1/8\pi(L/b)][(1+\nu)/(1-\nu)] - (kT/\mu b^3)$ , where  $a$  is the kink height as shown in Fig. 8.11. Taking  $a/\rho = 6$ ,  $\nu = \nu$  (copper) = 0.324, and  $kT/\mu b^3 = 1/400$ , then  $\sigma/\mu = 2.5\text{E-}5$  for  $L/b = 1\text{E}3$  and  $2.5\text{E-}4$  for  $L/b = 1\text{E}2$ .
- 15.7☆ Discuss the significance of the inception of amplitude dependence in a Bordoni peak experiment, in terms of the results of Prob. 15.6.  
 There is no amplitude dependence provided there is only one kink pair formed in the interval during one cycle. An amplitude dependence arises when more than one pair forms because there is a pair-pair interaction that influences the nucleation rate.
- 15.8☆ a. Consider a crystal that suddenly is subjected to an isostatic compressive stress  $P$  under isothermal conditions. Before the vacancy concentration changes, is there a super- or under-saturation  $c/c^0$  of vacancies according to the definition of  $c^0$  in Eq. 14.39?

Undersaturation. The pressure aids in the lattice contraction at the vacancy site and thus lowers the energy of formation.

- b. Will an edge dislocation in the crystal move transiently before a new equilibrium concentration is established?

Yes, there will be a transient climb driving force that vanishes when the vacancy concentration equilibrates.

- c. Derive the expression for the initial total force on the dislocation.

The dislocation moves up in Fig. 15.15a, thereby creating vacancies within the dislocation core. The climb force is given by Eq. 15.74, where  $c$  is given by the second equation after Eq. 15.76.  $c < c^0$ , in accord with example (a) above.

- 15.9 Consider a region of crystal with a pressure  $P + p$  and a vacancy concentration that is in equilibrium with local internal sources and sinks in that region. Is there a super- or under-saturation of vacancies in the region?

- 15.10 If internal sources and sinks are present, discuss the mechanism by which vacancy diffusion tends to diminish internal stresses.

- 15.11 Derive an expression for the time for a circular prismatic dislocation loop, formed by collapse of a vacancy disc, to shrink to one-half the original radius  $R$ .

- 15.12 ☆ Express Eqs. 15.135 and 15.136 in a general vector notation for  $\mathbf{v}$  in terms of a force produced by the stress tensor  $\boldsymbol{\sigma}$ .

In both equations, replace  $F/L$  by Eq. 3.95. The climb motion is in the  $(\mathbf{b} \times \boldsymbol{\xi})/|\mathbf{b} \times \boldsymbol{\xi}|$  direction.

- 15.13☆ a. Derive the growth velocity analogous to Eq. 15.108 for a square prismatic loop formed by vacancy disc collapse. Assume quasi-equilibrium with jogs everywhere on the dislocation line.

The exact solution is very difficult to obtain but the process is similar to that in Prob. 15.11. Eq. 15.108 provides an expression for the climb velocity,  $v = 2\pi C_1 S_0 / 4C'L$ , where  $C_1 = \mu D_s v_a / 2(1-v)kT$ ,  $C' = \mu b^2 / 4\pi(1-v)$ , and  $2\pi R$  is replaced by  $4L$  to equate the circumferences of the square and circular loops. The line tension is defined in Eq. 6.75 as  $S_0 = \partial W / \partial L$ , the variation in energy with respect to a change in length of dislocation loop.  $W$  for a square prismatic loop of edge length  $L$  is obtained using the procedure outlined in Prob. 6.3 and it takes the form:

$$W_{n=4 \text{ prismatic loop}} = C'L \left[ 4 \ln \frac{L}{ep} + C \right]$$

The  $\ln$  term represents the contribution from the self energy of the four edges and  $C$  captures the interaction energies between the four edges; it is not calculated in this example. The result is  $S_0 = C' \ln[(L/ep) + 1 + C/4]$ .

The line tension therefore takes the form  $S_0 \approx C' \ln(L/ep) \approx C' \ln(L/b)$ . The energy of the square is then  $4LS_0$ . Here,  $\partial N / \partial L = S_0 v_a / 2bL$ . The diffusion solution is the same and Eq. 15.106 becomes  $C' \ln(L/b)$ . Eq. 15.108 is then replaced by  $v \approx \pi D_s S_0 v_a C' \ln(L/b) / LkT$ . This is quite similar to Eq. 15.108.

- b. Note that the square shape of the loop suggests that geometric jogs are absent in growth because they grow out to the corners of the square and vanish. Discuss the mechanism of loop growth. What condition must occur for the quasi-equilibrium assumption of (a) to be valid?

The mechanism is kink pair nucleation and growth, the jog equivalent of Eq. 15.45. kink pair annihilation distance, pertinent to the mechanism of Eq. 15.43, must be close to  $L$  in order that quasi-equilibrium of vacancies along the line is approximately established. In the limit of a long waiting time between nucleation events, the vacancy concentration would drop below the local equilibrium value.

- c. When such a loop shrinks, the shape tends to be circular in contrast to a square (or more generally polygonal) growth shape. Discuss the reason for this difference in shape. There is a direct analog to this shape difference in the topography of crystal growth and dissolution (Frank and Ives 1960).

As the loop shrinks the interaction forces,  $\propto 1/L$ , become very large so that the nucleation barrier becomes quite small and the nucleation rate is quite large. The kink spacing is then so small that the line becomes essentially a circular shape. The circle, as opposed to other curves shapes, is stabilized kinematically by the diffusion process.

- 15.14 ☆ Discuss the situations analogous to that in Figure 15.29b where a vacancy is absorbed in the middle of the jog line and where a vacancy is absorbed at each end of the jog line at the same time.

The absorption in the middle is more difficult because it results in twice the number of jogs. Adsorption at one end when there is already a vacancy absorbed at the other end is more favorable because there is an elastic attraction force between the two jogs.

## CHAPTER 16: GLIDE OF JOGGED DISLOCATIONS

**Description:** These problems discuss the velocity of screw dislocations with jogs, creep rates, motion of superjogs, and the formation of jogs from intersection of dislocations.

- 16.1 a. Compute the value of  $\sigma$  for which Eq. 16.5 approximates Eq. 16.4 within 5% and also 1%. Assume silver at 800 °C with  $l = 100 b$ .
- b. Compute  $v$  for  $\sigma = 10^{-3} \mu$  at 800 °C. Assume  $D_s = a_0^2 v \exp(-W_s/kT)$ ,  $v = 10^{13} \text{ s}^{-1}$ , and  $W_s = 1.9 \text{ eV}$ . What creep strain rate does this  $v$  correspond to if the active dislocation density  $\rho = 10^8 \text{ cm/cm}^3$ ?
- 16.2 ☆ Assume an energy-displacement curve of the form of Figure 16.5 for vacancy formation at a jog. Compute  $W^*$  and  $a^*$  using

$$W(\sigma, x) = 1.5(W_v + W'_v) \left( 1 - \frac{10\sigma}{\mu} \right) \sin^2 \left( \frac{\pi x}{a} \right)$$

Compare the magnitudes of the various terms in Eq. 16.10 for this case.

Eq. 16.9 provides the definition for  $a^*$ . Set  $C(\sigma) = 1.5(W_v + W'_v)(1 - 10\sigma/\mu)$  so that  $W = C \sin^2(\pi x/a)$ . The result is  $\sin(2\pi a^*/a) = \sigma b l a / \pi C$ . If  $a^*/a$  is small, then  $a^* = \sigma b l a^2 / 2\pi^2 C$ . The terms in Eq. 16.10 are  $l a^*$ ,  $l a^*$ ,  $-l a^*$ . Here, the terms  $\partial C / \partial \sigma$  are assumed to be small compared to  $\partial a^* / \partial \sigma$ . The conclusion is that all three terms are comparable in magnitude.

- 16.3 ☆ a. How are the point forces at jogs in screw dislocations affected if the jogs are superjogs?

The point forces scale with the jog height if the superjog moves uniformly. The point forces would change little if the superjog advanced by a mechanism wherein unit jogs traverse the superjog.

- b. Derive the equation analogous to Eq. 16.7 for the superjog case.  
If the jog height is  $na$  where  $n$  is an integer and  $a$  is an atomic distance along the superjog, then Eq. 16.7 is modified by a factor  $n$  in the denominator.
- c. Describe a mechanism whereby superjogs can advance by single-vacancy emission. Draw the appropriate jog configurations.

Unit jogs traverse the superjog as discussed in Sec. 15.6 and as illustrated in Fig. 15.29.

- 16.4 Compute the critical stress for motion of vacancy-forming jogs without thermal activation, for silver with  $W_v \sim 1.0$  eV and  $W_i \sim 4$  eV. Do the same for interstitial-forming jogs. Compare these stresses with the that required to move a dislocation at a velocity of  $10^6$  cm/s (Eq. 16.18). Use  $l = 10^2 b$  and  $T = 800$  °C.

- 16.5 ☆ In a fcc material, consider an extended screw dislocation that intersects a *random* array of dislocations.

- a. What are the probabilities of forming acute and interstitial jogs?

For intersections with a random array, there would be equal numbers of acute or obtuse jogs as well as equal numbers of interstitial-forming and vacancy-forming jogs.

- b. Describe a mechanism by which an acute extended jog can become an obtuse extended jog.

The conversion can occur when the dislocation line rotates as in the sequence  $(a) \rightarrow (c) \rightarrow (b)$  in Fig. 10.19.

- c. Which type of jog is expected to predominate in an *equilibrium* array?

Acute jogs should dominate because of their smaller stair-rod Burgers vectors.

- 16.6 ☆ Along a screw dislocation, suppose that an acute extended jog is a superjog. Show mechanistically how such a jog can climb by single-vacancy absorption.

In Fig. 10.20a, a vacancy would form at the partial  $\alpha A$ . Since the jog-line is equivalent to a row of  $1/3$  vacancies, the dislocation advances by a distance  $3a$ , where  $a$  is the atomic spacing along the jog-line.

## CHAPTER 17: DISLOCATION MOTION IN VACANCY SUPERSATURATIONS

**Description:** These problems address the climb of dislocations upon up quenching, nucleation of vacancy loops upon quenching, operation of Bardeen-Herring sources with interacting arms, the formation of helical dislocations, the formation of jogs on stacking fault tetrahedra, and the interaction of concentric partial dislocation loops.

- 17.1 Consider a silver crystal with an edge dislocation along the axis of a right circular cylinder of radius  $R = 10^4 b$ . If the cylinder is rapidly up-quenched from room  $T$  to near the melting point, compute the maximum possible climb rate and the initial quasi-steady-state climb rate of the dislocation. Assume  $W_v = 1.0$  eV and  $W_v' = 0.9$  eV.
- 17.2☆ For an aluminum crystal quenched from 650 to 300 °C, compute the nucleation rate of circular prismatic  $\frac{1}{2}\langle 110 \rangle$  loops in the presence of normal stresses  $\sigma = 10^{-6}E$ ,  $10^{-4}E$ ,  $10^{-2}E$ , and  $10^{-1}E$ . Note the correction in the question statement (red text).  
**MATLAB.** Use Eq. 17.6 to estimate the steady-state nucleation rate  $J = Z\omega n_c$ , where  $Z \approx 0.1$  (see text following Eq. 17.6) and  $\omega$  and  $n_c$  are given by Eqs. 17.7 and 17.8, respectively. The discussion in Sec. 17.3b cites  $\Delta G^* = 3.25$  eV and this is lowered by  $\sigma b \pi r^{*2}$ , where the discussion provides an estimate,  $r^* = 4E-10$  m. Thus,  $\Delta G^*$  is lowered by 3.2E-5, 3.2E-3, 3.2E-1, and 3.2 eV for the four values of stress, assuming that the resolved shear stress =  $\frac{1}{2}$  applied normal stress and  $b = 2.89E-10$  m and  $E = 7.1E10$  Pa for aluminum. Eq. 17.8 predicts the equilibrium concentration of critical size loops to be  $n_c = 6.9E-1$ ,  $7.4E-1$ ,  $4.6E2$ , and  $1.1E28$  m<sup>-3</sup> for the four values of stress. Eq. 17.7 estimates the frequency at which vacancies join the loop,  $\omega = 2.6E2/s$ , based on an attempt frequency  $\nu = 1E13/s$  as adopted in Prob. 16.1b, a concentration  $c = 1.1E28/m^3$ , and  $W_v = 0.76$  eV and  $W_v' = 0.62$  eV from the discussion in Sec. 17.3b. The steady-state nucleation rate,  $J = Z\omega n_c$ , has values of 1.8E1, 1.9E1, 1.2E4, and 3.0E29 m<sup>-3</sup> s<sup>-1</sup> for the four values of normal stress. The results are consistent with the conclusion in the discussion that appreciable densities of loops (e.g., in Figure 17.1) require values of applied stress approaching the theoretical strength.
- 17.3 Compute the nucleation rate of circular, Frank partial, prismatic  $\frac{1}{3}\langle 111 \rangle$  loops after quenching from 650 to 300 °C, assuming  $\gamma_1 = 200$  mJ/m<sup>2</sup>. Compare the results to those of Prob. 17.2. Discuss the experimental observation of  $\frac{1}{3}\langle 111 \rangle$  faulted loops in high-purity quenched aluminum.

- 17.4 ☆ Suppose that one arm of an operative Bardeen-Herring source swings around several screw dislocations so that it passes over the opposite arm by three interplanar distances. Consider the likelihood of annihilation in such a case and also the resultant dislocation configuration.

The attractive interaction force is  $\mu b^2/6\pi a$ , where  $a$  is the atomic spacing normal to the plane of Fig. 17.5. The dislocations would annihilate under such a stress. The Bardeen-Herring mechanism applies only to planar arrays.

- 17.5 ☆ What forces act on a helical dislocation formed from a screw and lying normal to a free surface? What results when the helix glides into the surface? Assess the likelihood of such glide quantitatively.

The helix is of mixed screw-edge character. Image forces attract the helix, which moves by climb. However, the climb is conservative since opposite segments have opposite edge components. Hence, the overall process is glide of the helix to the surface by a conservative climb mechanism. The overall (thermodynamic) image force is the same as that for a straight screw parallel to the surface. The surface is locally sheared but its topography is unchanged when the helix glides out, just as for a straight screw. The likelihood of such glide is greater when the removal of dislocation energy,  $\mu b^2 \ln 2$ , near the surface is greater in magnitude than the energy,  $\gamma b$ , of the step, where  $\gamma$  is the energy/area of the step riser.

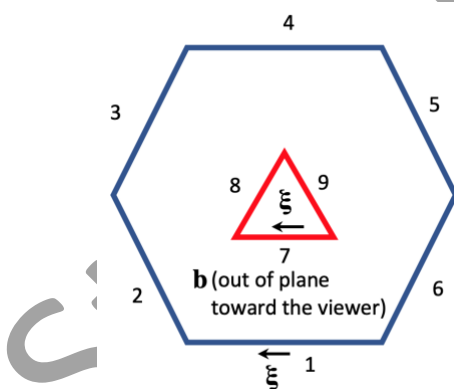
- 17.6 Consider a straight mixed dislocation line in an unstressed crystal. If an external isostatic pressure is applied to the crystal, show that the dislocation will initially tend to transform into a helical shape but will eventually straighten out. Discuss the forces acting on the dislocation at each stage.

- 17.7☆ Suppose a mixed dislocation transforms into a helical dislocation in the absence of net mass transport to or from the dislocation. Show that the helix formation requires both local core diffusion and net climb of the dislocation, *i.e.*, the axis of the helix is displaced from the original position of the straight dislocation. Compute the distance of climb as a function of  $\lambda$ ,  $r$ , and  $b_e$ .

As in Fig. 17.8, the helix is topologically equivalent to a straight dislocation and a set of prismatic loops. The latter can only correspond to an aggregate of either vacancies or interstitials. These can only be supplied by climb of the mixed dislocation. The number of loops per unit length of line is  $\lambda$  and the number point defects needed is  $\pi R^2/\lambda v_a$ . For climb by a distance  $L$ , the number of point defects produced is  $b_e L/v_a$ . Equating these results gives the answer.

- 17.8 Construct a sequence of diagrams showing the stages of the following:
- Formation of an acute jog line at a tetrahedron corner by vacancy emission.
  - Annihilation of an interstitial at an obtuse jog line on a tetrahedron.

- 17.9☆ Use the method of Chapter 6 to verify that a positive interaction energy results for a hexagonal Frank partial and a smaller, concentric triangular Frank partial. This means that the nucleation of such triangles is unfavorable and it indicates the possibility of heterogeneous nucleation.



Problem 17.9.

The stable form of a Frank loop is a circle, approximated as a hexagon in Chap. 6. Single Frank loops form by vacancy condensation under irradiation. The question is whether the nucleation of a second loop is more favorable than the formation of another single Frank loop.

The accompanying figure shows the geometry and interaction energy between the loops involves the paired terms:  $W_{71}$  and  $W_{74}$ ;  $W_{72}$  and  $W_{75}$ ;  $W_{73}$  and  $W_{76}$ .  $W_{71}$  involves the interaction of parallel, like-signed segments and therefore it is positive.  $W_{74}$  is negative but the segments are more separated than for  $W_{71}$ . Therefore, the sum  $W_{71} + W_{74}$  is positive. Likewise, the other pairs involve pairs with oppositely signed Burgers vector when the coordinate system of Figure 6.4 is imposed. The net result is a positive interaction energy between the hexagonal and triangular loops. Thus, a second loop at the same site is unfavorable and single loops should be favored, consistent with experimental observations.

## CHAPTER 18: EFFECTS OF SOLUTE ATOMS ON DISLOCATION MOTION

**Description:** These problems consider forces to move excess atoms in a potential well, creep velocities with interstitial carbon present, estimates of breakaway stress when dislocation cores are not fully saturated with solute, binding of a second phase to a dislocation core, and the effect of supersaturation of solutes on dislocation nucleation.

18.1 Show that Eq. 18.35 follows from Eqs. 18.11 and 18.36.

18.2 Compute the creep velocity in mild steel for  $\sigma \sim 10^{-4} \mu$  at  $T = 600$  K, according to Eq. 18.108. Assume that carbon equilibrates with cementite.

18.3☆ Use Eq. 18.72 to compute the creep velocity in mild steel for  $\sigma \sim 10^{-4} \mu$  at  $T = 600$  K. Assume that carbon equilibrates with cementite.

**MATLAB.** Similar to Prob. 18.2, the Peach-Koehler formula (Eq. 3.93) provides the thermodynamic force unit length,  $F/L = \sigma b$  on a dislocation arising from the applied stress. This is equated to the drag force/unit length provided in Eq. 18.72. The solution for the dislocation velocity is

$$v = \sigma b D / kT c_0 \beta^2 l(z_0) = \sigma b \omega / kT c_0 z_0^2 (r_0/b)^2 l(z_0)$$

The second equality is obtained by substituting  $D \approx b^2 \omega$  and  $\beta = kT r_0 z_0$ . The mean jump frequency  $\omega = \nu \exp(-G/kT)$ , where the activation energy for diffusion of carbon in BCC iron is 1.6 eV/atom (Wells et al. AIME **188**, 553 (1950)) and  $\nu = 10^{13}/s$  as used in previous problems.  $c_0$  is approximated by  $c_\infty$  for carbon in equilibrium with cementite, as described in Prob. 18.2.  $z_0 = W_{\max}/kT$  (Eq. 18.74) defines the maximum binding

energy of a solute atom to a dislocation, relative to  $kT$ , and  $l(z_0)$  is defined in Eq. 18.75. Substitution  $z_0 = 2$ ,  $r_0 = b$ , and the other quantities into the above equation for velocity gives the answer,  $v = 1.5E-16$  m/s. This answer is relevant to a Cottrell atmosphere, where drag is associated with the translation of solute atoms with the dislocation, as it moves.

- 18.4☆ Assume that  $W_B \gg kT$  but  $c_0$  is low so that the core is not saturated. Generalize the theory of Sec. 18.5 to describe such conditions. In particular, derive the equations equivalent to Eqs. 18.124, 18.129, and 18.130.  
The equations are the same but  $W_B$  is replaced by  $XW_B$ , where  $X$  is the fraction of core sites occupied by solute.
- 18.5☆ Discuss the possibility of using the results of Prob. 18.4 to construct a theory for amplitude-dependent internal friction in very dilute substitutional alloys.  
The value of  $L$  in Fig. 15.12 is limited by solute pinning to the spacing between solute atoms in the core, which can be appreciable in the dilute limit. There is then a spectrum of values of  $L$  for the kink-pair model of Sec. 15.3b. As the stress increases, larger lengths have the configuration of Fig. 15.12 at the critical frequency, leading to an amplitude dependent internal friction.
- 18.6 The stress field of a dissociated pure screw dislocation interacts with impurities. Will logarithmic divergence arise as discussed in Sec. 18.3? Derive an approximate formula for the Cottrell drag in this case.
- 18.7☆ Consider Cottrell drag for an edge dislocation in an  $AB$  alloy that is not dilute. Discuss what diffusion coefficient should be used in this case.  
The diffusivity is that of the solute  $B$  alone. The bulk diffusivity depends on the diffusion coefficient for both  $A$  and  $B$ , but here only the diffusivity of the solute  $B$  is relevant. The Cottrell model is inapplicable once the atom fraction of  $B$  exceeds  $\sim 0.20$ . A new theory is needed for greater  $B$  concentrations.
- 18.8☆ Discuss qualitatively how binding *between* core impurities might affect the critical stress for dislocation breakaway from the core solute.  
For a fixed bulk concentration of solute, such binding would increase the number of empty sites on the core, make it easier to create solute free lengths, and decrease the breakaway stress.
- 18.9 Vacancies can form a Cottrell atmosphere about a dislocation according to Eq. 14.45. Compute the drag force produced by such an atmosphere on a screw dislocation and compare the results to Eq. 16.4. Is it justified to neglect the second-order Cottrell atmosphere effect in this case?

- 18.10 ☆ Discuss the various factors that contribute to the binding of a dislocation to a tube of second phase precipitated on the dislocation. Calculate the binding energy as a function of displacement for the case of the hollow dislocation core (Prob. 3.9).

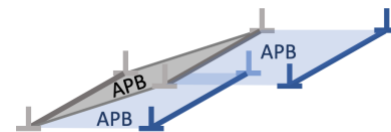
Consider the screw case. There is a modulus effect, giving an interaction energy:  $(\Delta\mu b^2/4\pi) \ln(R_p/r_0)$ , where  $\Delta\mu$  is the mismatch in elastic shear modulus and  $R_p$  is the radius of the cylindrical precipitate.  $\Delta\mu = \mu$  for a void (a second phase of zero modulus). The dislocation is smeared into a continuous distribution of infinitesimal dislocations on the interface and the self-energy is reduced to  $(\mu b^2/4\pi) \ln(R/R_p)$ . The results for the edge are analogous with  $\Delta[\mu/(1-\nu)]$  replacing  $\Delta\mu$  and with a factor  $(1-\nu)$  added to the self-energy.

- 18.11 Consider the possibility that Suzuki type locking is caused by vacancies at an extended dislocation in a pure metal.

- 18.12 ☆ Estimate the order of magnitude binding energy between a solute and dislocation to achieve spontaneous dislocation generation in a supersaturated solid solution.

If a dislocation loop of radius  $R$  formed, the energy would be  $W_s = \mu b^2 R \ln(R/r_0)$  and the amount of solute would be reduced by the number of solutes in the core,  $N = \pi R^2 a/\Omega$ , where  $a$  is the atomic spacing normal to the loop and  $\Omega$  is the atomic volume. For a saturated core, this process lowers the energy by  $W = 2\pi R W_B N(1-X)$ , where  $X$  is the solute volume fraction in the matrix. When  $W \geq W_s$ , spontaneous generation of dislocations is possible.

- 18.13 Compute the drag force for the glide motion of the configuration in Figure 18.24a.



Problem 18.13.

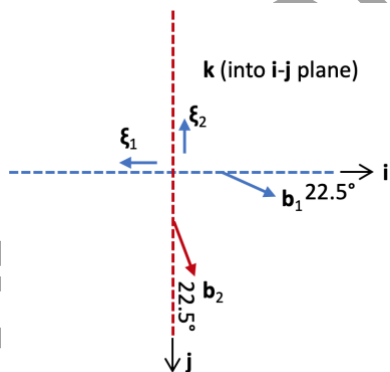
## CHAPTER 19: GRAIN BOUNDARIES AND INTERFACES

**Description:** These problems consider dislocation descriptions of simple tilt, twist boundaries as well as boundaries formed by specific slip systems, stress fields from grain boundaries, interactions between dislocations and boundaries, and forces on boundaries generated by an applied stress.

19.1 Derive  $\mathbf{N}_1$  for a simple tilt boundary consisting of one set of edge dislocations.

19.2 Determine  $\mathbf{N}_1$  and  $\mathbf{N}_2$  for a simple twist boundary consisting of two sets of orthogonal screw dislocations.

19.3☆ Consider two sets of dislocations with Burgers vectors that are inclined to one another at  $45^\circ$ . Determine  $\mathbf{N}_1$  and  $\mathbf{N}_2$  for a pure twist boundary in their common glide plane. What is the dislocation density in the two sets for an angle of rotation  $\theta$ ?



Problem 19.3.

The two sets of dislocations are drawn as pure screw dislocations as shown in the accompanying figure, with reference axes  $\mathbf{i}$ ,  $\mathbf{j}$ ,  $\mathbf{k}$ , and Burgers vectors  $\mathbf{b}_1$  and  $\mathbf{b}_2$  rotated by  $22.5^\circ$  so that the angle subtended by the Burgers vectors is  $45^\circ$ . Eq. 19.43 applies, consistent with the case of two sets of dislocations where the rotation axis  $\mathbf{a} \parallel (\mathbf{b}_1 \times \mathbf{b}_2)$ . Also,  $\mathbf{n} \cdot \mathbf{b}_1 = \mathbf{n} \cdot \mathbf{b}_2 = 0$  so that the result is:  $\mathbf{N}_1 = (\sin 22.5^\circ \mathbf{i} + \cos 22.5^\circ \mathbf{j})/b_1(\cos 45^\circ)$  and  $\mathbf{N}_2 = (\sin 22.5^\circ \mathbf{i} + \cos 22.5^\circ \mathbf{j})/b_2(\cos 45^\circ)$ . Using Eq. 19.20,  $N_1 = \sqrt{2}/b_1$  and  $N_2 = \sqrt{2}/b_2$  and Eq. 19.19 furnishes the dislocation densities  $1/D_1 =$

$N_1 2 \sin(\theta/2)$  and  $1/D_2 = N_2 2 \sin(\theta/2)$ , where  $\theta$  is the angle of twist (Figure 19.15a). In any equilibrium boundary with fixed Burgers vectors, the lines of dislocations can be rotated in this manner.

19.4☆ A grain boundary in a simple cubic crystal system is composed of the dislocations  $\mathbf{b}_1 = [1\ 0\ 0]$ ,  $\mathbf{b}_2 = [0\ 1\ 0]$ , and  $\mathbf{b}_3 = [0\ 0\ 1]$ . Determine  $\mathbf{N}_1$ ,  $\mathbf{N}_2$ , and  $\mathbf{N}_3$  when

$$\mathbf{a} = \frac{1}{\sqrt{14}}[123], \quad \mathbf{n} = [100]$$

What are the directions of the dislocations? What are the dislocation densities when  $\theta = 5^\circ$ ?

This is an interesting problem in that it entails the inadequacy of the independent slip system concept when interfaces with significant rotations are present. The independent slip system concept is exact when the dislocations have a nominally uniform distribution (see UF Kocks, CN Tomé, HR Wenk, *Texture and Anisotropy*, Academic Press, New York, 2000). Additional systems may be required when rotations are involved, as at grain boundaries, twins, or shear bands. This is the case here: the methods of Chapter 9 would imply that they are only two independent systems. However, for the present case, only  $\mathbf{b}_1$  can contribute to tilt rotation since  $\mathbf{b}_2$  and  $\mathbf{b}_3$  lie in the boundary and only  $\mathbf{b}_2$  and  $\mathbf{b}_3$  can contribute to twist since  $\mathbf{b}_1$  is normal to the boundary. Hence, the boundary is special in that it is a superposition of a tilt boundary with a single Burgers vector and a twist boundary requiring two Burgers vectors, even though they would be classified as independent in the Chapter 9 methodology.

The rotation of  $5^\circ$  can be split into a twist rotation about the  $x$ -axis of  $\alpha = 2.67^\circ$ , a tilt rotation about the  $y$ -axis of  $\beta = 4.00^\circ$ , and a tilt rotation about the  $z$ -axis of  $\gamma = 1.33^\circ$ .

For the twist contribution about the  $x$ -axis, the screw dislocations are orthogonal with  $\xi \parallel \mathbf{b}_3$  and  $\mathbf{b}_2$ , and rotated by  $1.34^\circ$  with respect to each grain, giving the relative twist of  $\alpha = 2.67^\circ$ . For the tilt about the  $y$ -axis,  $\xi \parallel \mathbf{e}_y$ , the Burgers vector is  $\mathbf{b}_1$ , and the tilt angle is  $\beta = 4.00^\circ$ . For the tilt about the  $z$ -axis,  $\xi \parallel \mathbf{e}_z$ , the Burgers vector is  $\mathbf{b}_1$ , and the tilt angle is  $\gamma = 1.33^\circ$ .

The dislocation densities are given by Eq. 19.5 as follows. For the twist boundary, both screw sets have  $N_1 = 0.0465/b$ . For the tilt about the  $y$ -axis, the result is  $N_2 = 0.0349/b$ . For the tilt about the  $z$ -axis,  $N_3 = 0.016/b$ .

There are two features here that are of general interest. First, the intersecting (dependent) edge sets would react at nodes and combine into one slant set of edges, since they have the same Burgers vector. The formalism of grain boundary theory yields a possible solution. There are always possible reactions of this combining type or the formation of a three-fold network as for twist boundaries on  $\{1\ 1\ 1\}$  planes in fcc. Second, while a twist boundary of the above type probably has minimum energy, the twist could also comprise edge or mixed dislocations (see J. P. Hirth (1993) "Stabilization of Strained Multilayers by Thin Films" *J Materials Research* 8: 1572-77). With some elastic anisotropy cases, the edge or mixed configurations could have lower symmetry. Also, they could exist as metastable arrays as a consequence of the formation process.

- 19.5☆ What boundaries in a NaCl-type structure can form by glide if the only active slip systems are  $[1\ 0\ 1](1\ 0\ \bar{1})$  and  $[1\ 0\ \bar{1}](1\ 0\ 1)$ ?

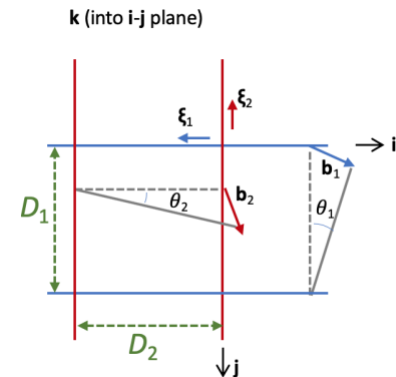
Eq. 19.40 applies for the case since  $\mathbf{p}_1 \times \mathbf{p}_2$  and  $\mathbf{b}_1 \times \mathbf{b}_2$  are collinear. In such cases, the discussion following Eq. 19.39 indicates that any boundary plane parallel to  $\mathbf{b}_1 \times \mathbf{b}_2$  ( $= [0\ 1\ 0]$ ) is possible.

19.6 What boundaries in a NaCl-type structure can form by glide if the only active slip systems are  $[1\ 0\ 1]$  ( $1\ 0\ \bar{1}$ ) and  $[1\ 1\ 0]$  ( $1\ \bar{1}\ 0$ )? Is this a realistic case?

19.7☆ Generalize the example of Figure 19.34 to fcc tilt boundaries formed by glide on intersecting slip planes.

A simple example would be  $\mathbf{BA}(d) + \mathbf{DB}(a) \rightarrow \delta\mathbf{A}(d) + \mathbf{D}\alpha(a) + \alpha\delta$ . The long-range field is that of a tilt wall of  $\mathbf{DA}$  dislocations. The  $\alpha\delta$  stair-rods have tilt character. The other partials have components parallel to the tilt plane but they are equal and opposite. The product is a Lomer-Cottrell barrier. See Chap. 22.

19.8 Derive the stress distribution around the boundary of Prob. 19.3. Show explicitly that no long-range stresses exist.



Problem 19.8.

19.9☆ Demonstrate that the general theory for grain boundary energies (Sec. 19.7) agrees with the results of Prob. 19.8. Calculate the values of  $F_j$  and  $F_j''$  for that example and discuss the limiting behavior as  $X_j \rightarrow 0$ .

The interaction force between grain boundary  $A$  and a segment of length  $\ell_1$  in grain boundary  $B$  is depicted in Figure 19.40. For the grain boundary in Prob. 19.8, the stress field for each set of screw dislocations is given by Eqs. 19.85, where  $X = x/D$  and  $Y = y/D$  are reduced coordinates parallel and perpendicular to an array. The force/unit length on a segment is given by the Peach-Koehler formula (Eq. 3.93) and in general it does

not decay with increasing normalized distance,  $Y$ , from the boundary. However, the superposition of the stress fields from sets 1 and 2 does decay with increasing  $Y$  provided  $b_1/D_1 = b_2/D_2$ . That is the case for Prob. 19.8. An approximate form for the decay, Eq. 19.94, explicitly shows that the interaction force drops rapidly (exponentially) for distance larger than the dislocation spacing in the boundary. This result demonstrates St. Venant's principle.

- 19.10 What type of applied stress tensor could cause a pure twist boundary to glide
- In the most general case?

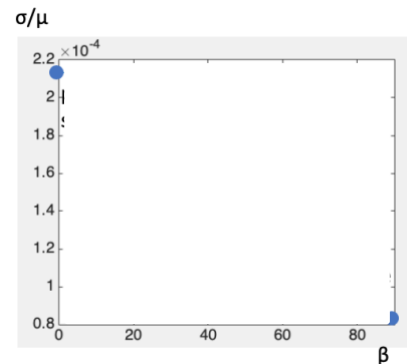
- When the sets of dislocations in the boundary are pure screw.

- 19.11 ☆ Consider the interaction of a single dislocation  $DC(a)$  when it intersects the pure twist boundary composed of the pure screws  $AB$ ,  $BC$ , and  $CA$  on glide plane ( $d$ ) in an fcc crystal.

## CHAPTER 20: DISLOCATION SOURCES

**Description:** These problems consider estimates of yield strength, prismatic loops and hexagonal meshes as sources, the effect of stress on the activation energy of to operate a bowed loop as a source, the effect of interaction between bow outs and surface ledges on source operation.

- 20.1 Estimate the critical resolved shear stress to yield a crystal with a dislocation network of average segment length  $l = 10^4 b$ .



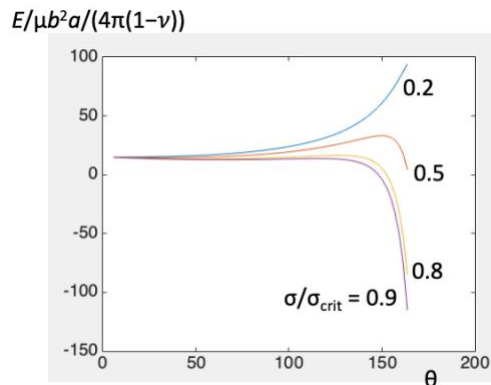
Problem 20.1.

20.2 Consider a prismatic loop that has formed by vacancy condensation on a (1 1 1) plane in a fcc structure and that has reacted so that no stacking fault is present in the plane of the loop. Can this loop be a source for slip? If so, specify the planes and slip directions.

20.3☆ A source consists of a pure twist boundary of screw segments in a hexagonal mesh on a (1 1 1) plane in an fcc crystal. Which slip systems can operate from it?

Figure 10.9 and the accompanying Thompson tetrahedron (Fig. 10.10) show that the hexagonal mesh would be comprised of screw dislocations along  $\langle 1\ 1\ 0 \rangle$  directions. Each screw dislocation could cross slip onto another {1 1 1} plane, e.g., a screw dislocation **CB** along  $[\bar{1}\ 0\ 1]$  could cross slip from plane (d) to plane (a). Likewise, **CA** could cross slip from (d) to (b) and **BA** from (d) to (c). Thus, three slip systems could operate by cross slip, in addition to the three slip systems on the parent (1 1 1) plane.

20.4☆ For  $\sigma < \sigma_{crit}$ , compute the stable and metastable equilibrium positions of a bowed loop with the geometry in Figure 20.1. Determine the activation energy to achieve the latter from the former. Show that the process is unlikely under thermal activation unless  $\sigma \sim \sigma_{crit}$ .



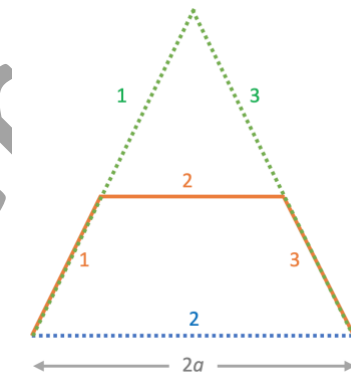
Problem 20.4.

**MATLAB.** Consider a bowed loop of radius  $R$  as shown in Figure 20.1, where  $2a$  is the distance between the ends of the bowed loop (*i.e.*, the pinning sites), and  $d\theta$  in the image is replaced by  $\theta$ . If a resolved shear stress  $\sigma$  acting on the slip plane in the direction of slip is present, then the energy to introduce the loop into a stress-free body is  $E_{loop} = 2R\theta\mathcal{S}$ , where the line tension  $\mathcal{S}$  is approximated by  $[\mu b^2/4\pi(1-\nu)]\ln(2a/\rho)$ . See Eq. 20.1. The work of the applied shear stress acting through the relative slip  $b$  and over the area that is sheared when the dislocation bows from a straight segment to one with radius  $R$  is  $W_{applied\ stress} = \sigma b R^2 [2\theta - \sin(2\theta)]$ . The total energy is  $E_{total} = E_{loop} - W_{applied\ stress}$ . The variable  $R$  can be replaced by  $a/\sin\theta$  and  $E_{total}$ , normalized by  $\mu b^2 a / 4\pi(1-\nu)$  is  $W_{total(norm)} = (2\theta/\sin\theta)\ln(2a/\rho) - (\sigma/\mu)2\pi(1-\nu)(a/b)(2\theta - \sin(2\theta))/\sin^2\theta$ .

The accompanying figure shows  $W_{total(norm)}$  as a function of  $\theta$  for  $a/b = 1E3$ ,  $\rho/b = 1$ , and the following values for copper:  $\mu = 5.46E10$  Pa,  $\nu = 0.343$ , and  $b = 2.54E-10$  m. For

reference,  $\mu b^2 a / 4\pi(1 - \nu) / kT = 2.6E4$  at room temperature and  $\sigma_{crit} = S/bR = 8.9E-4 \mu$ . The accompanying plot shows the normalized total energy for  $\sigma/\sigma_{crit} = 0.2, 0.5, 0.8,$  and  $0.9$ . Even at  $\sigma/\sigma_{crit} = 0.9$ , the activation energy, which is the difference in  $W_{total}$  at the unstable equilibrium (in the vicinity of  $\theta \sim 150^\circ$ ) and  $W_{total}$  at the stable equilibrium location (in the vicinity of  $\theta = 60^\circ$ ) is  $\sim \mu b^2 a / 4\pi(1 - \nu) \sim 3E4 kT$ . This activation energy is too large to be thermally accessible. At  $\sigma_{crit}$ , the activation energy is zero. Thus, the activation energy is  $\sim kT$  only when  $\sigma \sim \sigma_{crit}$ .

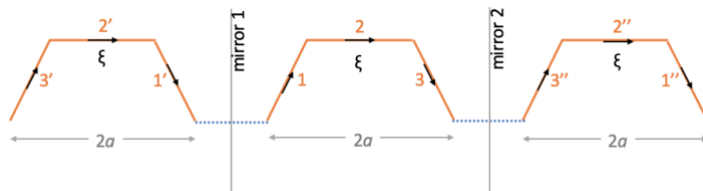
- 20.5 Use the straight segment methods of Chapter 6 to compute the degree of bow out as a function of stress for a loop constrained to have its component segments in  $\langle 110 \rangle$  directions on a  $\{111\}$  plane in germanium, as in Figure 20.2. Compare the results with those of Eq. 20.1. Assume that the original unbowed segment is pure screw.



Problem 20.5.

- 20.6☆ For pinned segments that are uniformly spaced along a screw dislocation, compute the contribution of interaction between adjacent loops to the bow out energy for the loops. Assume the loops are composed of straight segments, as in Prob. 20.5.

It suffices to consider three adjacent semi-hexagonal bow-outs as shown in the accompanying figure. The middle loop would interact with the other two. A primary issue is whether the interaction would increase or decrease the energy  $W_{loop}$  of the center loop. The interaction energy between segments on opposite sides of “mirror plane 1” and “mirror plane 2” will be positive and negative, e.g.,  $W_{11'} < 0$  is expected since segments 1 and 1' have the same  $\mathbf{b}$  but the in-plane components of  $\xi_1$  and  $\xi_{1'}$  are oppositely signed. Conversely,  $W_{13'} > 0$  since the segments are parallel and have the same  $\mathbf{b}$  and  $\xi$ .



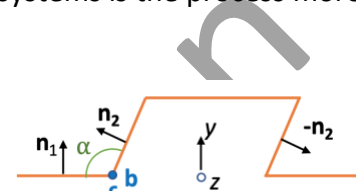
Problem 20.6.

$W_{11'}$  is expected to have a larger magnitude than  $W_{13'}$  due to the smaller distance between interacting segments and thus the effect of

the neighboring segments is expected to decrease  $W_{loop}$ . This ought to decrease  $W_{total}$ , particularly as the loops extend toward the inverted “V” shape (green dashed lines shown in Prob. 20.5) and  $W_{11'}$  grows in magnitude relative to  $W_{13'}$ . This is expected to decrease the applied stress and activation energy to expand a loop.

- 20.7 ☆ Consider the formation of a closed dipole loop by the mechanism of Figure 20.5f. Show that the relative resolved shear stress makes formation less likely in a fcc crystal compared to a simple cubic crystal. For which other crystal systems is the process more likely?

If the resolved shear stress favors the initial cross-slip, it disfavors the final cross slip. Thus, the final step is more favorable after unloading, whereupon the interaction energy would favor the final (secondary) cross-slip. Also, if the proper stress gradient were present, the final cross slip event might occur more easily. These effects would be exacerbated in the simple cubic case since the relative resolved shear stress on the cross slip plane is larger (equal to that on the primary plane).



Problem 20.7.

To demonstrate, the accompanying figure shows a primary slip plane with  $\mathbf{n}_1 \parallel y$  axis =  $[1\ 1\ 1]$  and  $\mathbf{n}_2 = [1\ 1\ \bar{1}]$ . A screw dislocation with  $\mathbf{b}$  and  $\xi \parallel z$  axis =  $[\bar{1}\ 1\ 0]$  resides at the intersection of these planes. A shear stress  $\sigma_{yz}$  will favor glide of the screw dislocation to the right and a portion of  $\sigma_{yz}$ , of magnitude  $\sigma_{yz} (\mathbf{n}_1 \cdot \mathbf{n}_2)$ , will drive the first cross slip event. The portion,  $\sigma_{yz} (\mathbf{n}_1 \cdot -\mathbf{n}_2)$  to drive the second cross slip event on the  $-\mathbf{n}_2$  plane is therefore reversed and thus the second event would be disfavored by the applied stress. For the FCC geometry here,  $\alpha \approx 108^\circ$  and thus  $\sigma_{yz}$  will have an asymmetric effect, favoring one cross slip event while disfavoring the other. For a cubic system, the applied  $\sigma_{yz}$  is symmetric; it produces no resolved component on the first and second events. For the fcc case, the asymmetric nature can make formation of the double cross slip more difficult.

In systems such as hexagonal or monoclinic where the angle between the primary and cross-slip planes can be small, the process would be favored.

- 20.8 *Singular* surfaces are perfect low-index surfaces while *vicinal* surfaces are near a low-index orientation and contain surface ledges and surface kinks. On which type of surface is dislocation nucleation more likely? For which type of surface is edge dislocation reflection by the Frank mechanism more likely? Why?

## CHAPTER 21: DISLOCATION PILEUPS

**Description:** These problems examine the calculation of equilibrium positions in pile-ups and the length and number of dislocations in pile-ups. Applications are made to determine the stress field around cracks, including the effects of free surfaces, and also to precipitates.

21.1 Consider a glide pileup of three edge dislocations that form against a barrier under an applied resolved shear stress  $\sigma$ . Assume the leading dislocation is fixed and calculate the positions of the second and third dislocations relative to it.

21.2☆ Suppose that the frictional stress on the glide plane is  $\sigma_f$ . Determine the length of a single-sign glide pileup of  $N$  edge dislocations if no applied stress is present.

The formalism for the single-sign pile-up under an applied stress  $\sigma$  (Sec. 21.5) can be used except that  $\sigma$  is replaced by  $\sigma - \sigma_f$  when a frictional stress is present. Accordingly, Eq. 21.36 is used with  $\sigma - \sigma_f$  replacing  $\sigma$ . Upon unloading,  $\sigma - \sigma_f \rightarrow 0$  and then upon further unloading,  $\sigma$  takes on the value  $\sigma_f$ . Thus, the length of the pile-up is  $\ell = \mu Nb / [\pi(1 - \nu)\sigma_f]$ .

21.3☆ Use the preceding problem to estimate dislocation core widths. Assume that the critical shear stress for slip of a perfect crystal is  $\mu/20$ .

The resolved shear stress on the partials differs. The one with the larger shear stress  $\sigma$  will move first and must overcome the attractive force provided by the fault to break away. Thus, in Eq. 21.36,  $N = 2$ ,  $\sigma$  is replaced by  $\gamma/b + \mu b/20$ , and  $\mathbf{b}$  is the Burgers vector of the partial.

21.4 The shear stress to operate a source of edge dislocations is  $\sigma^*$ . A barrier exists at a distance  $L$  in front of the source but not in the rear. How many dislocations will pile up behind the barrier if a resolved shear stress  $\sigma > \sigma^*$  is applied? What is the resultant force on the barrier?

21.5 A microcrack grows and fractures a brittle solid at a tensile stress  $\sigma = 10^{-3} \mu$ . Estimate the size of the microcrack if the surface energy  $\gamma = \mu b/10$  and Poisson's ratio  $\nu = 1/3$ .

- 21.6 ☆ A surface source of screw dislocations operates at a negligibly small stress and forms a pileup forms at a distance  $L$  below the source. Estimate the force on the obstacle under an applied stress  $\sigma$ .

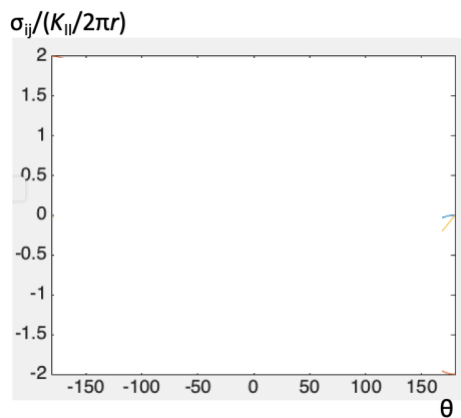
The force at the tip is that of a pile-up of length  $L_p$  plus that of the image pile-up. To first-order, the image stress is that of a superdislocation with Burgers vector  $Nb$  at position  $(-L_p, 2L)$  with the pileup tip at  $(0, 0)$ . More precisely, the image field is given by Eqs. 21.51 and 21.52.

The single pile-up in the vicinity of a free surface can be approximated by a double pile-up in an infinite body, as shown in Figure 21.5. The position  $x = 0$  in Figure 21.5b is the location of the free surface, with positive dislocations for  $x > 0$  and negative (image) dislocations for  $x < 0$  (see also Figure 3.16 for the image construction). The force per unit length in the double pile-up is given by Eq. 21.21 for a double pile-up of edge dislocations, except that the  $(1 - \nu)$  factor is omitted, consistent with the different expressions for the stress field for edge and screw dislocations (Eqs. 3.3 and 3.45). The result is  $F/L = \pi \sigma^2 \ell / 4\mu$ . For comparison,  $F/L$  for a single pile-up from a source far from a free surface is obtained from  $F/L = N\sigma b$ , where  $N$  is given by Eq. 21.35. The result,  $F/L = \pi \sigma^2 \ell / \mu$ , is larger than that for the surface source.

- 21.7 ☆ Derive the equivalent of the Griffith criterion for a tensile crack whose surface is normal to a free surface. Use the analogy with Prob. 21.6.

Now the image tip position is at  $(0, 2L)$  and the procedure is the same as that in the previous problem.

- 21.8 Determine the plane of maximum normal stress ahead of an edge dislocation glide pileup.



Problem 21.8.

- 21.9 Use a continuum theory to verify that a pure tilt boundary composed of a single set of uniformly spaced edge dislocations has no long-range stress field. Do long-range stresses occur if the dislocations are not uniformly spaced?
- 21.10☆ Show how the results of this chapter can be used to determine the stress field around a coherent, plate-shaped precipitate.  
Suppose the precipitate is a circular disc of radius  $r$  and thickness  $d$  in the  $z$ -direction. The atomic spacing differs in the  $z$ -direction so part of the field is that of a prismatic dislocation loop at the disc periphery with  $\mathbf{b} = (0, 0, b_z)$  and a magnitude equal to the difference in  $z$  spacing. The coherency stress involving differences in atomic spacing parallel to the plane of the disc must be computed separately. In special cases, line force fields may be needed, see Hirth et al (2016a) with corrections in (2017).

## CHAPTER 22: DISLOCATION INTERSECTIONS AND BARRIERS

**Description:** These problems consider: the interaction forces between dislocations and their relaxations under glide and climb; dislocations and jogs associated with reactions, cross slip, and dissociation; and the extension of barriers.

- 22.1☆ Compute the distribution of interaction force between two orthogonal edge dislocations, separated by a distance  $h$ , each with its Burgers vector parallel to the line of the other dislocation.  
Consider the geometry in Fig. 22.3, where the line directions for dislocations  $A$  and  $B$  are along the  $x$  and  $y$  directions, respectively. However, there are two edge dislocations, with  $\mathbf{b}_A$  oriented along the  $y$ -direction and  $\mathbf{b}_B$  oriented along the  $-x$  direction. Dislocation  $A$  will experience a glide force,  $F_y/L = \sigma_{zy}^{B \rightarrow A}(x, z = h)b_A$ , and a climb force,  $F_z/L = -\sigma_{yy}^{B \rightarrow A}(x, z = h)b_A$ , where the notation  $B \rightarrow A$  denotes the stress generated by dislocation  $B$  at the site of dislocation  $A$ . The stress components  $\sigma_{zy}^{B \rightarrow A}(x, z = h)$  and  $\sigma_{yy}^{B \rightarrow A}(x, z = h)$  can be expressed as  $\sigma_{y'z'}(-x', y = h)$  and  $\sigma_{z'z'}(-x', y = h)$ , where the  $x', y', z'$  coordinate system is that used in Figure 3.10. According to Eqs. 3.45,  $\sigma_{y'z'} = 0$  and thus no glide force is exerted by  $B$  on  $A$ . However,  $\sigma_{z'z'}(-x, y = h) = -C h/(x^2 + h^2)$ , where  $C = \mu b v / \pi(1 - \nu)$ . Therefore, a climb force  $F_z/L = C b h/(x^2 + h^2)$  is exerted on  $A$ . This is largest at  $x = 0$ . Likewise, dislocation  $B$  has a climb force  $F_z/L = -\sigma_{xx}^{A \rightarrow B}(y, z = -h) = -C b h/(x^2 + h^2)$ .
- 22.2 Indicate how the two dislocations in Prob. 22.1 would relax if (a) only glide is allowed and (b) both climb and glide are allowed.

- 22.3☆ Consider interactions in bcc crystals that yield dislocations of the  $\langle 1\ 0\ 0 \rangle$  type. Classify these interactions in terms of the screw-edge character of the reacting dislocations and the line direction of the product dislocation. If the  $[0\ 0\ 1]$  dislocation is glissile on  $(1\ 1\ 0)$  and  $(1\ \bar{1}\ 0)$  but sessile on other planes, which reactions yield sessile  $[0\ 0\ 1]$  dislocations? Attractive junctions would be of the type  $\frac{1}{2}[1\ 1\ 1] + \frac{1}{2}[1\ \bar{1}\ \bar{1}] = [1\ 0\ 0]$ . Unlike the fcc case, the attractive junction forms for all screw-edge characters. All other combinations of  $\frac{1}{2}\langle 1\ 1\ 1 \rangle$  Burgers vectors are unstable.
- 22.4☆ Consider the possibility that an *intrinsically* dissociated screw dislocation cross slips into an *extrinsically* dissociated screw through an intermediate state analogous to that in Figure 22.18d. Would this be an easier cross-slip process than that in Figure 22.18d if  $\gamma_E$  were only slightly larger than  $\gamma_I$ ? Use the Frank  $b^2$  criterion for the energy of the partials. What reservations exist concerning the application of the Frank criterion? The partial loop would bulge downward with the Burgers vector now being  $\delta A$  and the fault being extrinsic. The smaller stair-rod would energetically favor this reaction according to the Frank criterion but nucleation might still be less favorable because of the larger core. A more accurate analysis would treat the screw-edge character using an expanded Frank criterion. The screw-edge character differs for the trailing partials in the two cases.
- 22.5☆ Derive the extrinsically faulted barriers corresponding to barriers (1) to (4) in Figure 22.12. The equivalent for barrier 1 would be the configuration of Fig. 22.10 rotated by  $\pi$  in the page. The trailing partials would be  $D\alpha$ , upper left, and  $\delta A$ , upper right. A similar procedure, with shape inversion, works for the other barriers.
- 22.6 Assume a tensile stress acts along  $[0\ 0\ 1]$  in a NaCl-type crystal. Verify that the dislocation jogs formed by intersections between the  $[\bar{1}\ 0\ 1](1\ 0\ 1)$  and  $[0\ \bar{1}\ 1](0\ 1\ 1)$  slip systems are interstitial-forming.
- 22.7 Assume that the operation of a slip system is proportional to the resolved shear stress on it. For fcc tensile tests, show that barriers (1) and (4) are favored to form when the tensile axis is near  $[2\ 1\ 1]$ , while barriers (2) and (3) are favored for orientations near  $[1\ 2\ 0]$ . In both cases, the axes lie within the unit stereographic triangle  $[1\ 0\ 0]$ ,  $[1\ 1\ 0]$ ,  $[1\ 1\ 1]$ .
- 22.8☆ Verify that the equilibrium configuration of barrier (5) in Eq. 22.6 should be asymmetric. Note the correction in the question statement (red text). The equilibrium configuration is asymmetric because  $\alpha C$  and  $B\gamma$  are mixed. Hence, compared to symmetric barriers, they have smaller forces that depend only on their edge components.

22.9 Which barriers in Table 22.1 can be considered extended in a meaningful sense? How does this result affect the pileup size that a barrier can sustain if  $\langle 1\ 1\ 0 \rangle \{0\ 0\ 1\}$  slip easily occurs in fcc?

22.10☆ Draw the product barrier of Eq. 22.5 if it extends to form an obtuse angle barrier. Identify the types of faults in the barrier. Note the correction in the question statement (red text).

The dislocation **DB** now enters from the top. See Fig. 22.10 (right). The partial  $\delta\mathbf{A}$  remains the same but the trailing partial  $\alpha\mathbf{B}$  is at the upper left, the stair-rod is **BD**/ $\alpha\delta$ , and the upper fault is extrinsic.

## CHAPTER 23: DEFORMATION TWINNING

**Description:** These problems consider: candidate twin planes; estimates of the stress in the vicinity of a twin; influence of stress components on twinning, growth or shrinkage of twins; and dislocation interaction with twins.

23.1☆ In principle, could  $(1\ \bar{1}\ 0)$  be a twin plane in a fcc crystal?

No. The  $(1\ \bar{1}\ 0)$  plane already has mirror symmetry.

23.2 Consider a twin lamella of thickness  $h$  formed by  $\frac{1}{6}[1\ 1\ 1]$  glide on  $(1\ 1\ \bar{2})$ , the  $K_1$  plane. What is the superdislocation at the spearhead of the twin? Estimate the stress at a distance  $\sim h$  ahead of the spearhead, assuming no emissary glide has occurred.

23.3☆ Consider the same twin as in Prob. 23.2, but it is formed by Bullough's mechanism. Are the stresses at the spearhead different in this case?

The Bullough case is depicted in Figure 23.3b, where the twin is formed by slip on planes  $K_2$  in a direction parallel to  $\eta_2$ . The difference is highly localized, only within a distance equal to the dislocation spacing in the Bullough case. If the shear is imparted but the local rotation is suppressed, there will be small differences in the local strain. See the reference for Hirth, Pond, and Lothe (2006) in the textbook.

23.4 Do compressive stresses normal to  $K_1$  influence twinning if it proceeds as assumed in Prob. 23.2? As in Prob. 23.3?

23.5 Are shear stresses other than that resolved on the twinning plane and in the twinning direction important for twin nucleation in the models of Figures 23.7a and 23.7b?

23.6 Discuss why the concept of a critical resolved shear stress for twinning might be inadequate. Problems 23.4 and 23.5 are relevant to this question.

23.7☆ Consider Figure 23.16. During annealing, should the twin shrink or grow to consume the entire slipped zone? Why?

The twin should slowly grow or shrink until it is bounded on the top and bottom by  $\{1\ 1\ 2\}$  twin planes. The weak driving force for this slow process is the decrease in surface area of the twin, reflected locally by an attraction of twinning disconnections with oppositely signed steps.

23.8☆ Derive the possible reactions for  $\frac{1}{2}\langle 1\ 1\ 0 \rangle$  type dislocations that glide through coherent twin interfaces in fcc crystals and leave partials in the boundary.

Consider a  $(1\ 1\ 1)$  twin plane. For all such reactions, the product and reactant Burgers vectors have a component  $\frac{1}{3}[1\ 1\ 1]$  normal to the twin plane and an in-plane component of the type  $\frac{1}{6}\langle 1\ 1\ 2 \rangle$ . Thus, all residual vectors are sums of two  $\frac{1}{6}\langle 1\ 1\ 2 \rangle$  vectors. One class is of the form  $\frac{1}{6}[\bar{1}\ 2\ \bar{1}] + \frac{1}{6}[1\ 1\ \bar{2}] = \frac{1}{2}[0\ 1\ \bar{1}]$ . All other combinations result in products that are partials. Also, the defect could remain in the boundary. An example would be a  $\frac{1}{2}[1\ 1\ 0]$  reacting to form a sessile  $\frac{1}{3}[1\ 1\ 1]$  partial dislocation or a disconnection and a glissile partial  $\frac{1}{6}[1\ 1\ \bar{2}]$ .